Cretaceous Research 144 (2023) 105430

Contents lists available at ScienceDirect

Cretaceous Research

journal homepage: www.elsevier.com/locate/CretRes

New advances in the stratigraphy of Aptian oceanic anoxic events (Castro Urdiales, Basque-Cantabrian Basin, Spain)

Pedro A. Fernández-Mendiola [a], Joanaitz Pérez-Malo [a, *], Hugh G. Owen [b, †], Joaquín García-Mondéjar [a]

[a] Department of Geology, Faculty of Science and Technology, University of the Basque Country (UPV/EHU), Bilbao, Spain
[b] Department of Earth Sciences, The Natural History Museum, London, UK

ARTICLE INFO

Article history:
Received 1 March 2022
Received in revised form
17 October 2022
Accepted in revised form 18 November 2022
Available online 30 November 2022

Keywords:
Black shale
Aptian
Oceanic Anoxic Events
Volcanism
Basque-Cantabrian Basin

ABSTRACT

The Aptian sedimentary deposits of the Castro Urdiales area in north Spain record an episode of disoxia/anoxia which postdates Oceanic Anoxic Event 1a (OAE 1a). Carbonate platform and overlying facies are analysed for stratigraphy, sedimentology, total organic carbon and carbon isotopes. Lower Aptian shallow-water limestones are covered by deeper-water marlstones and organic-carbon-rich black lutites of lower to upper Aptian, ranging from *Dufrenoyia furcata* Zone to *Cheloniceras (Epicheloniceras) martinioides* Zone. Biostratigraphy and chemostratigraphic calibration are based on ammonites, carbon isotopes and total organic carbon analyses, revealing consistency with the global Aptian reference framework. The Castro Urdiales black-shale levels of the lower to upper Aptian transition together with their encasing series are correlated with other Aptian sections of the Basque-Cantabrian Basin (northern Spain) and southeastern France. The Castro Urdiales black shales are correlated with the Aparein Level of the eastern Basque-Cantabrian Basin. Prior to this oxygen deficient episode, glauconite-and-ostreid facies were also deposited under oxic conditions during the Gutiolo volcanic event of the Basque-Cantabrian Basin. This volcanism correlates in part with the Cretaceous superplume eruptions of Ontong Java, Manihiki Plateaus and the North Atlantic opening as a result of increasing seafloor spreading rates.

1. Introduction

Organic-carbon-rich black shales constitute source rocks for petroleum and natural gas, thus being of great interest both geologically and economically (e.g., Ohkouchi et al., 2015). Black shales are deposited in marine realms at different geologic periods, not exclusively, but often during phases of widespread oxygen depletion referred to as Oceanic Anoxic Events (OAEs). OAEs are intensively investigated to constrain the mechanisms and feedback processes guiding oceanographic, biological and climatic changes. Several ocean-wide anoxic/dysoxic episodes have been reported for the Aptian, which interrupted the marine sedimentation under normal oxic conditions. The main anoxic phase in the Aptian is known as Oceanic Anoxic Event 1a (OAE 1a). It is recorded as organic-carbon-rich sediments in land sections from around the world and DSDP/ODP sites in the North and South Atlantic, Indian and Pacific Ocean Basins (e.g., Bralower et al., 1994; Castro et al., 2019; Fu et al., 2020; Giorgioni et al., 2015; Giraud et al., 2018; Hu et al., 2012; Naafs and Pancost, 2016; Schlanger and Jenkyns, 1976; Tejada et al., 2009; Wang et al., 2016; Weissert and Erba, 2004). OAE 1a is identified at a variety of palaeodepths ranging from shallow-water environments down to more than 4.5 km depth (e.g., Hueter et al., 2019; Jenkyns, 2010, 2018; Pancost et al., 2004; Westermann et al., 2013). It was modulated by the local depositional environment in terms of local geography, bathymetry, climate, ocean chemistry, nutrient supply and biological communities. After several decades of research, many questions still remain open concerning the determination of the local versus global factors influencing the organic matter (OM) enrichments, and understanding the environmental constraints on OM production and preservation.

The recognition of early Aptian OAE 1a and associated episodes of OM accumulation is of considerable importance in the study of the Early Cretaceous (e.g., Bottini and Erba, 2018; Gradstein et al., 2004; Hay, 2017; Jenkyns, 2010; Li et al., 2008). OAE 1a lasted

* Corresponding author.
E-mail address: joanaitz.perez@ehu.eus (J. Pérez-Malo).
† Hugh G. Owen passed away in March 2022, after completion of this manuscript but before its publication.

https://doi.org/10.1016/j.cretres.2022.105430

1–1.5 Ma and was a complex episode (Beil et al., 2020; Jenkyns, 2018; Pancost et al., 2004; Westermann et al., 2013). It was preceded and succeeded by periods of intermittent oxygen deficiency during the Aptian (Bralower et al., 1994). A series of additional subpeaks of anoxia occurred after OAE 1a both in the late early Aptian (e.g., Aparein Level of the Aralar Mountains, García-Mondéjar et al., 2009) and throughout the first half of the late Aptian (e.g., Niveau Noir and Niveau Fallot of the Vocontian basin; Bréhéret, 1997). Coeval episodes are also documented in the South Atlantic Cape Basin (Dummann et al., 2021). Additionally, the Wezel Level of the Umbria Marche Basin (central Italy) has also been recently highlighted as occurring after OAE 1a (Matsumoto et al., 2021). Integrating the precise stratigraphic range of these black-shale levels is a challenge for future research. In this research we describe the signature of inedit black-shale levels of the Castro Urdiales section (northern Spain) to allow comparisons within the Basque-Cantabrian Basin (BCB) and prospectively with worldwide basins. It is worth exploring the supraregional relevance of the Aptian rock record of the Basque-Cantabrian Basin.

The goal of this paper is to report the sedimentary sequence in Castro Urdiales and attempt a correlation with other published sections of the BCB that include both the OAE 1a and succeeding anoxic levels. The Castro Urdiales section exposes a thick sedimentary sequence with relevant palaeogeographic, palaeoclimatic and palaeoecologic information for stratigraphic correlation purposes. An integrated biostratigraphic, lithostratigraphic and geochemical research is conducted to elucidate the origin and spatio-temporal relationships of the sedimentary sequence, and discuss the local versus global forcing factors. Thus, investigation of carbon-rich deposits in regions like the BCB is important to furthering our understanding of Aptian black shales. The OAE 1a and the Aparein black-shale interval are marker horizons within the BCB. Intra and extrabasinal correlations have been proposed (Fernández-Mendiola et al., 2018; García-Mondéjar et al., 2009, 2015a,b; Millán et al., 2009). The OAE 1a and Aparein Level bear organic-carbon-rich levels and C isotope signals that can be used to help deduce local versus global driving factors. Additionally, discrepancies regarding the age of the Aparein Level, late early Aptian (Fernández-Mendiola et al., 2018, 2021) or late Aptian (Frau, 2021a,b), are reviewed and new data sheds light on this issue. The role played by disoxia/anoxia in the evolution of carbonate platforms is also addressed herein. Several triggering factors of environmental change in carbonate platforms have been suggested, including oxygen-deficient waters, tectonism, volcanism and sea-level changes (e.g., Christie-Blick, 1991; Christie-Blick et al., 1990; Church and Gregory, 2001; Gold, 2021; Haq et al., 1987; Kendall and Schlager, 1981; Vail et al., 1977). The volume of mid-ocean ridges, variations in spreading rates, mantle dynamics, convection in Earth's interior, superplumes, emplacement of large igneous provinces and variations in ice volume are additional drivers of paleoceanographic and paleoclimatic changes (e.g., Bottini et al., 2012; Larson and Erba, 1999; Méhay et al., 2009; Midtkandal et al., 2016; Miller et al., 2005; Tarduno et al., 1991; Tejada et al., 2009). Our study aims to contribute to the advancement of the understanding of the local (regional) versus global impact of paleoenvironmental changes.

2. Geological background

The Aptian sedimentary succession of Castro Urdiales lies in the central part of the BCB (Fig. 1A). In the Aptian, a pericratonic basin developed in the southern margin of the Bay of Biscay proto-oceanic rift (Montadert et al., 1979). Subsidence variations related to strike-slip movements induced the formation of: 1) zones of lesser subsidence capped by carbonate platforms and 2) more subsident zones with sedimentation of intra-platform siliciclastics. The stratigraphic arrangement was thus influenced by active fault-block activity (García-Mondéjar, 1990; Pascal, 1985; Rat, 1988). Major plate reorganisation characterised the Cretaceous as a result of the break-up of Gondwana, which was accompanied by a major marine transgression (Haq et al., 1987). The northward extension of the North Atlantic led eventually to the splitting of Iberia from the original European French western margin. This rearrangement influenced the BCB evolution. Global rising of sea level affected the Lower Cretaceous rift basins including the BCB (Fluteau et al., 2007). In this scenario, local tectonic events often played a role in the demise of carbonate platforms (e.g., Kendall and Schlager, 1981; Nelson, 2013). There is consensus that over long-time scales, sea level has been controlled by ocean-floor spreading and associated tectonics (e.g., Christie-Blick et al., 1990). The sedimentary sequences of the various sections over the BCB reflect the tectonic activity of rifting associated with the progressive northward opening of the North Atlantic and the Bay of Biscay from the Late Jurassic to the Early Cretaceous (e.g., Le Pichon and Sibuet, 1971; Malod and Mauffret, 1990) (Fig. 1). During the Aptian, the BCB underwent tectonic segmentation and extensional faulting resulting in development of horst/graben block patterns. These faults controlled differential subsidence and caused strong thickness variations in the sedimentary record (e.g., García-Mondéjar et al., 2004). The sedimentologic analysis of the Castro Urdiales succession can help to decipher the history of carbonate platform evolution and test the function played by synsedimentary tectonism and sea-level variations on environmental changes. Stratigraphic sections in the Castro Urdiales area were previously described by Rosales et al. (1994) and Rosales (1995, 1999) with Aptian-Albian facies mapping and stratigraphic/sedimentologic and sequence stratigraphic documentation. The section located south of Castro Urdiales in the Sagrado Corazón hill is here reviewed and updated on the basis of new sections analyses, sampling and ammonite biostratigraphy. Results of geochemical signals across the upper lower Aptian and basal upper Aptian of Castro Urdiales are published herein for the first time.

3. Materials and methods

The Castro Urdiales stratigraphic section was logged and measured using a classical Jacob's staff, hand lens analysis of polished sections and thin-section determination of petrologic textures through cross-polarized microscopy. The following stratigraphic intervals were sampled:1) the exposed topmost Ereza Formation, from which only the last metres were considered, 2) the Sagrado Corazón Formation (250 m), 3) the Cérdigo Formation (9 m), and 4) the basal 43 m of the El Haya Formation (Figs. 1B and 2). Sampling was performed at regular intervals of 4 m in the Sagrado Corazón Formation and every 2 m in the Cérdigo and El Haya formations. A total of 74 samples were collected (57 from micritic limestones and 17 more from the overlying wavy calcarenites, silty marlstones and lutites, Fig. 2) and carefully processed for geochemical analyses. The most fine-grained portion of each sample was separated by a handled micro-drill from cut rock faces avoiding the sparry cement, vein material and skeletal components.

All the samples were analysed in order to build a carbon isotope curve, ascertain the carbon isotope trends and allow for prospective correlations with standard curve trends (e.g., Menegatti et al., 1998). The 57 micritic limestone samples of the Sagrado Corazón Fm lack any geochemical/sedimentological indicator of diagenetic alteration, but they formed in platform interior environments which have been considered as settings with usually good preservation of the original carbon isotope signal (Tendil et al., 2019). Inorganic carbon isotope determinations were carried out in the Laboratory of Services for Research Assistance from University of A Coruña (Spain).

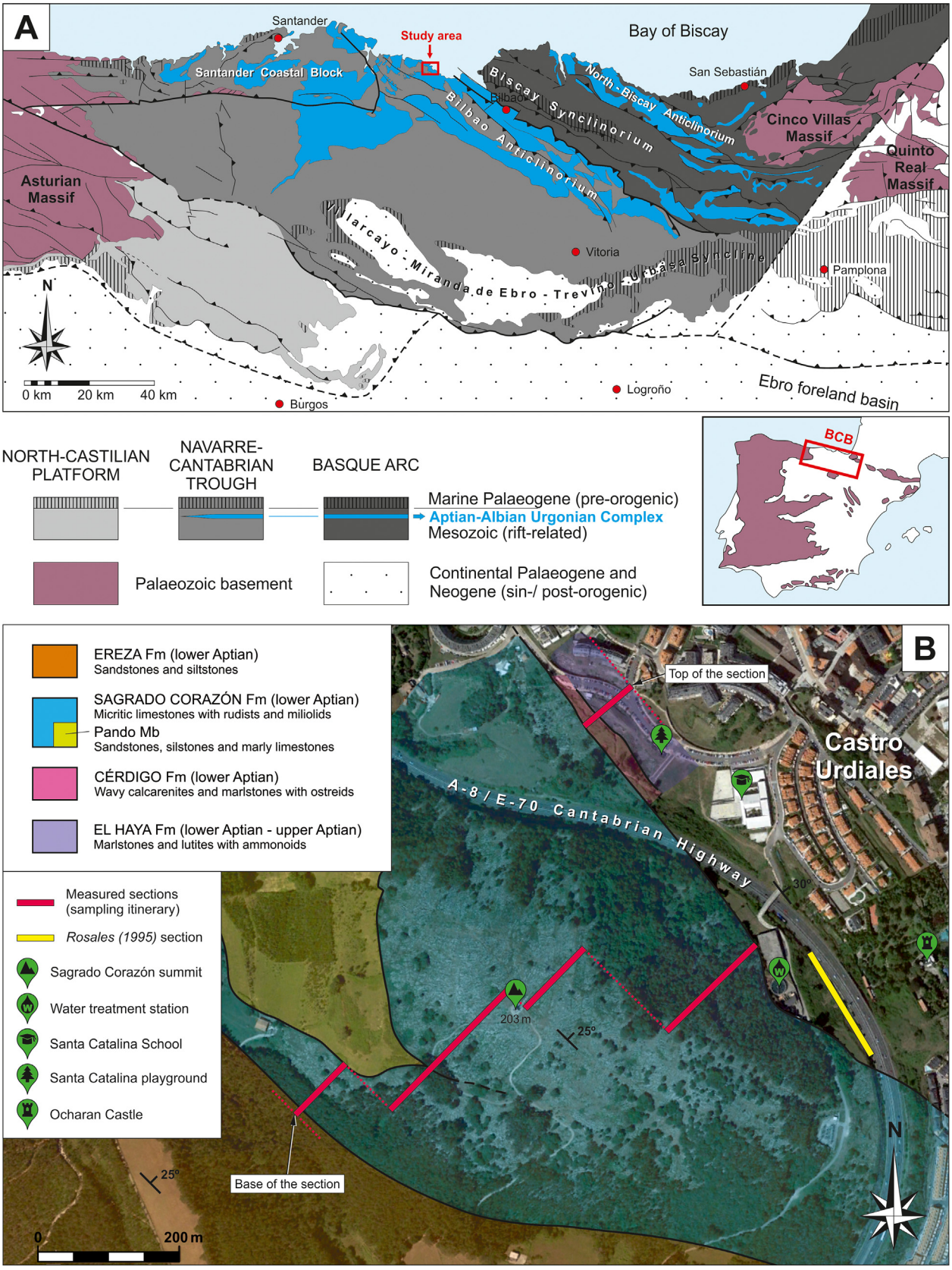

Fig. 1. A) Simplified geological map with the structural domains of the BCB (North Spain), showing the Aptian-Albian sin-rift deposits in blue (from Pérez-Malo et al., 2017). The study area lies in the Navarre-Cantabrian Trough, to the northwest of the Bilbao Anticlinorium. B) Top view of the study area, in which the Sagrado Corazón – Castro Urdiales School section outline and the stratigraphic formations are highlighted. Bedding gently dips homoclinally towards the northeast. (For interpretation of the references to colour in this figure legend, the reader is referred to the Web version of this article).

More than 5 g of sample material were treated with HCl acid (2 M) during 24 h to remove any carbonate minerals completely. Samples (300 μg) of decarbonated powder were weighed in 12 ml tin capsules and later treated with helium. 100 μl of orthophosphoric acid 99% (H_3PO_4) were added to each sample and they were kept at 26 °C for 24 h. The generated CO_2 was separated in a Poraplot Q column (25m, 0.32 mm, Varian) held at 70 °C. The system was calibrated with NBS19, NBS18 and LSVEC (IAEA, Vienna, Austria). Determinations were performed using a GasBench II (ThermoFinnigan) linked to a MAT253 mass-spectrometer. The reproducibility of the measurements based on replicate standards was 0.1% for $\delta^{13}C$. Additionally, organic carbon isotope results were obtained by means of a FlashEA1112 (ThermoFinnigan) elemental analyzer linked to a Deltaplus (ThermoFinnigan) mass-spectrometer. The samples were acidified with HCl before the analysis in order to eliminate the inorganic carbon fraction. The system was calibrated with USGS40, USGS41a, NBS22 and USGS24. Both inorganic and organic carbon isotope relations were expressed as per mil (‰) deviation from the Vienna Pee Dee Belemnite (VPDB).

Total organic carbon (TOC) was also measured with the aim of identifying organic-carbon-rich intervals that could point to anoxic conditions in the sedimentary environments. 74 samples were treated with HCl at 80% to dissolve carbonate minerals and 15 mg of powder was taken (%wt). The samples were introduced within a FlashEA1112 Elemental Analyzer calibrated against the standards, aspartic acid and urea. Precision of the analyses for replicate samples and standards was ±0.03%. These analyses were made in the Laboratory of Assistance for Research Services from University of A Coruña (Spain).

The Castro Urdiales School section was calibrated by means of ammonite biostratigraphy. A total of 25 newly discovered specimens (22 ammonoids and 3 nautiloids) were collected and examined in the Natural History Museum of London to help improve the biostratigraphy of the section (Fig. 3). The ammonite collection described in Rosales (1995) was also revised and updated. The whole collection, mainly composed of *in situ* found specimens, is currently housed in the University of the Basque Country (UPV/EHU, Bilbao, Spain).

4. Results

4.1. Litho- and biostratigraphy

The studied sedimentary succession is exposed adjacent southwest of Castro Urdiales village (Fig. 1B). The bottom of the section lies in the southern slope of the Sagrado Corazón hill (43°22′29.0″N, 3°14′05.9″W), whereas the top of the section is near the Castro Urdiales School (CEIP Santa Catalina) in Las Rozas neighbourhood (43°22′45.7″N, 3°13′25.3″W). The full profile is shown in figure 2, highlighting stratigraphic beds, facies and ammonite/nautiloid occurrences within the studied units. Four lithostratigraphic formations were formerly recognised (Rosales, 1995; Rosales et al., 1994), which will be described below in ascending order: Ereza Fm, Sagrado Corazón Fm, Cérdigo Fm and El Haya Fm. Recent excavation for house building in Castro Urdiales just west of the Santa Catalina CEIP (Castro Urdiales School), has produced a new outcrop for the Cérdigo Fm and the base of El Haya Fm. These units are laterally equivalent to the Castro Urdiales-2 section of Rosales (1995), which is located 500 m southeast of the Castro Urdiales School section (Figs. 1B, 3).

4.1.1. Ereza Formation

The Ereza Fm was defined by García-Mondéjar (1982) and formed in a shallow siliciclastic marine platform environment. The estimated thickness in Castro Urdiales is 875 m (Rosales, 1995). The Ereza Fm contains the record of the OAE 1a in the nearby sections of the Bilbao area (Fernández-Mendiola et al., 2018). It is laterally equivalent to the Errenaga Fm to the east of the BCB, where the OAE 1a was also reported (García-Mondéjar et al., 2009) and to the OAE 1a expression in the Patrocinio Fm to the west of the BCB (García-Mondéjar et al., 2015a,b; Najarro et al., 2011). In all these coeval Fms the OAE 1a geochemical signal is recognised and has served as a ground basis for intrabasinal correlation purposes. Based on this evidence it is proposed that the Ereza Fm might very likely encompass the OAE 1a in Castro Urdiales but this issue is beyond the scope of the present report, partly owing to the poor quality of the outcrops (Fig. 1B). The calcareous sandstones containing benthic foraminifera (mainly orbitolinids) of Ereza Fm in Castro Urdiales (Fig. 2) were deposited in a shallow-marine coastal environment subject to terrigenous input from continental source areas (e.g., García-Garmilla, 1987; Rosales et al., 1994).

4.1.2. Sagrado Corazón Formation

The Sagrado Corazón Fm is a 217-m-thick limestone unit of early Aptian age, based on the presence of *Praeorbitolina cormyi*, *Praeorbitolina wienandsi*, *Palorbitolina lenticularis*, *Chofatella decipiens* and *Iraquia simplex* (Rosales, 1999). It is laterally equivalent of: 1) the Galdames and Peñascal Fms (Fernández-Mendiola et al., 2018; Rosales, 1999), 2) limestone patches of the same age recorded in Gorbea (Zamburu and Arralde patches, 50 km eastwards (Fernández-Mendiola and García-Mondéjar, 1989) and 3) the limestone of the Sarastarri Fm in the Aralar Mountains, 100 km eastward of Castro Urdiales (García-Mondéjar et al., 2009). At the base of the Peñascal limestones a specimen of *Cheloniceras meyendorfi* records the upper *furcata* Zone of the lower Aptian (Fernández-Mendiola et al., 2018), and constrains the earlier attribution of *deshayesi-furcata* Zone to the Formation (Rosales, 1999). The geological mapping of the Sagrado Corazón limestones reveals an extension over 30 km and the limestone forms a series of patchy coeval lithosomes extending further west and east of the Castro Urdiales area (Rosales, 1995; Rosales et al., 1994). The Sagrado Corazón limestones intertongue laterally with deeper-water marlstones and sandstones (Rosales, 1995; Rosales et al., 1994). The lowest 10 m of the Sagrado Corazon Fm exhibit wavy-bedded calcarenites with abundant orbitolinids. The wavy-bedded character is marked by the occurrence of wispy clayey laminations. The calcarenites are skeletal packstones to grainstones composed of fine-sand-sized and poorly-sorted skeletal debris of echinoderms and bivalves. They represent the first carbonate facies of the section and correspond to the inception phase of the carbonate platform. The calcarenites suggest intermittently energetic conditions in a shallow sea affected by marine tractive currents, whereas the fine clays reflect phases of low hydrodynamic conditions with suspended terrigenous clay input derived from terrestrial source areas.

The overlying succession from metre 10 to 227 consists of well-bedded micritic limestone strata (Fig. 2). The micritic limestones contain abundant miliolid foraminifera, requieniid rudists and occasional corals and gastropods. The dominance of large and unbroken rudist shells in living position suggest *in situ* formation in low energy environment with trapping of fine mud matrix and infiltration of mud into intraskeletal voids. The carbonate muddy interval indicates shallow-marine quiet water environments with inner platform low-energy biotas. Similar rudist-rich mudstones to wackestones have been interpreted as being deposited in the photic zone at depths between 10 and 20 m (e.g., Hughes, 2000). Orbitolinids are also found in certain calcarenite horizons scattered throughout the section.

Several discontinuity surfaces have been recognised within the Sagrado Corazón limestones. The most significant discontinuity occurs at metre 87 of the Castro Urdiales section (Fig. 2). It shows an

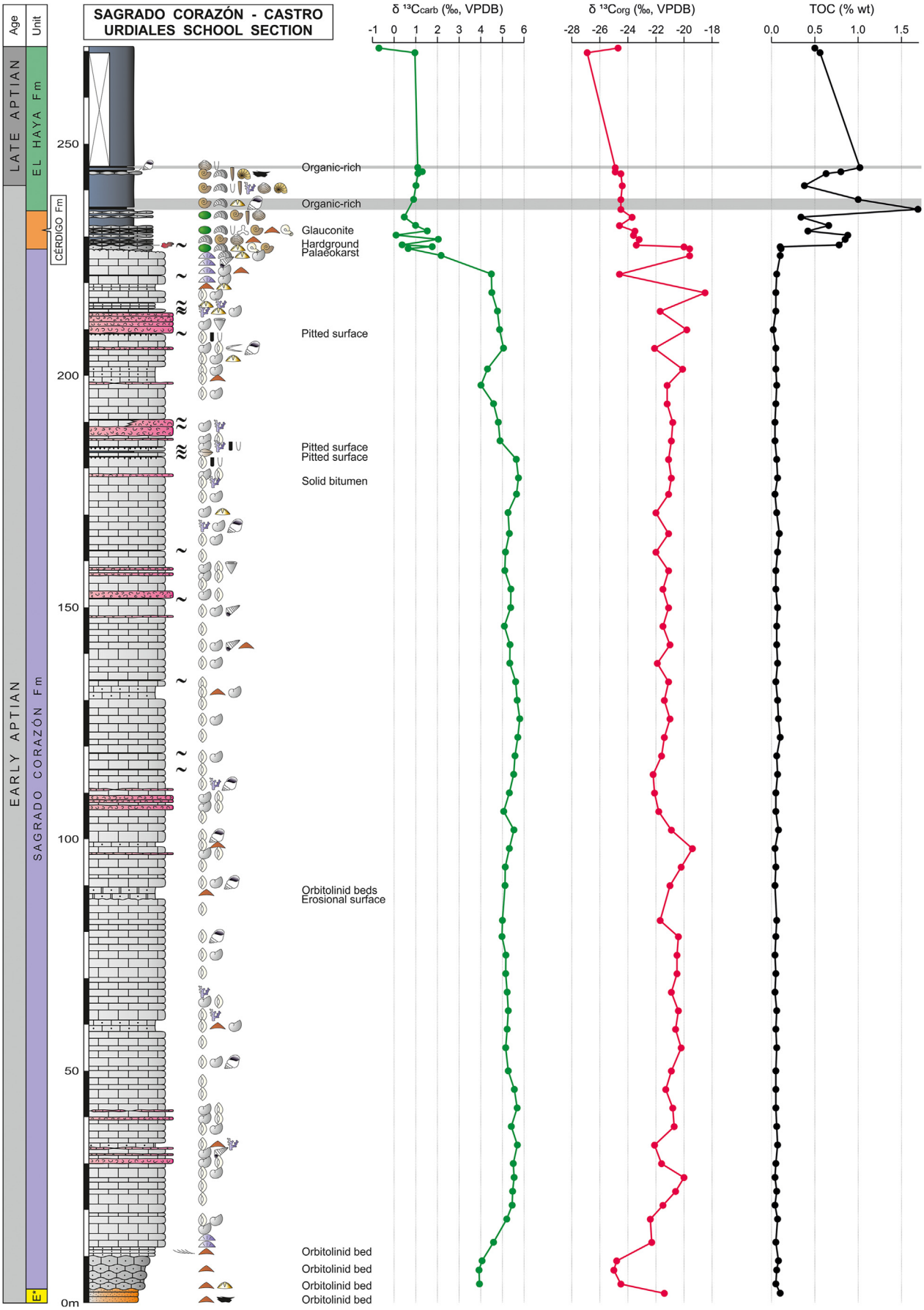

Fig. 2. Sagrado Corazón – Castro Urdiales School section highlighting the stratigraphy and facies, combined with $\delta^{13}C_{carb}$, $\delta^{13}C_{org}$ and TOC curves.

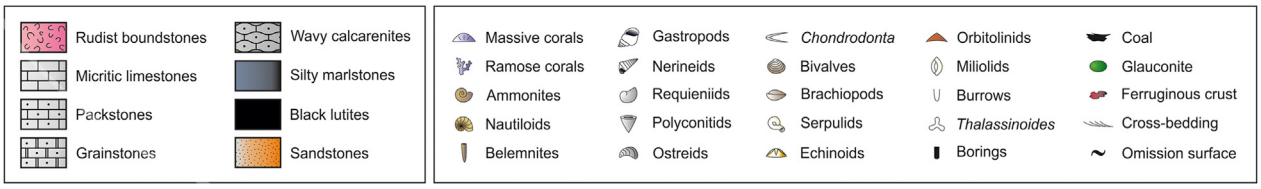

Fig. 2. (*continued*).

erosional character and evolves laterally northwestwards to the Pando Member siliciclastic wedge (Rosales, 1995) (Fig. 1B). This member is made up of lutites, marlstones and sandstones that display cross-bedding and local herringbone sedimentary structures with abundant siltstone laminae among the sandstone layers, suggesting cyclically alternating periods of strong currents and calm waters. This terrigenous wedge was deposited in a tidally influenced estuarine setting adjacent to the carbonate platform, in a more subsident and slightly deeper-water trough (Rosales, 1995).

The classical reciprocal sedimentation model, which typically includes shut-off of carbonate production and maximum accumulation rates of siliciclastics during sea-level lowstands (e.g., Catuneanu et al., 2011; Sarg, 1988; Schlager et al., 1994; Wilson, 1967), could be applied to the stratigraphic relationships observed in the western margin of the Sagrado Corazón lithosome (Fig. 1B). There are no tongues of limestone wedging towards the terrigenous trough. Instead, the Pando Member seems to onlap the Sagrado Corazón limestones. This is indicative of the absence of carbonate production during periods of siliciclastic sedimentation. In the studied section orbitolinid grainstones directly overlie miliolid wackestones, suggesting higher energy conditions of transgressive deposits succeeding the erosional discontinuity (Fig. 2).

Three significant omission surfaces with boring structures are also documented. They occur as well-defined bedding planes that display abundant subrounded hole structures forming pitted surfaces (metres 182, 185 and 209 of figure 2). The average size of the pits is 6 cm in diameter and their depth ranges from 3 to 5 cm. The origin of these sedimentary features is related to a hiatus in sedimentation and/or mechanical/biological erosion of early lithified limestone in very shallow-waters, thus representing a short break in the stratigraphic record (e.g., Clari et al., 1995). Discontinuity surfaces in carbonate strata are generally considered as either the result of erosion, subaerial exposure and/or a hiatus in sedimentation leading to lithification of the sea floor, or some combination of them (Clari et al., 1995; Hillgärtner, 1998; Sattler et al., 2005). The Castro Urdiales pitted surfaces are interpreted as incipient shallow-water hardgrounds. The stratigraphic distribution of discontinuities may exhibit systematic groupings. That is, rather than randomly distributed through the section, clusters of similar surfaces (erosional, omission or exposure) occur together at specific intervals. The upper part of the Sagrado Corazón Fm shows a greater concentration of omission surfaces, which suggests an overall upward-shallowing trend in the limestone succession.

A replacement in sedimentological facies is observed at metre 220 (Fig. 2), where the predominant rudist-miliolid association is replaced by coral-dominated micritic limestones (metres 220 to 227). Coral facies are often reported in deeper water than rudist biotopes, for instance, along the flanks of carbonate buildups in the lower Aptian of Saudi Arabia (e.g., Al-Ghamdi and Read, 2010). In the Castro Urdiales platform, the above described vertical sequence also indicates a final deepening trend towards more open marine conditions. The top of the Sagrado Corazón Fm is a disconformity with palaeokarst dissolution structures with up to 15–30 cm of palaeorelief (metre 227 of figure 2). This rugged surface with irregular holes records a period of subaerial exposure of the carbonate platform before being filled and covered by wavy calcarenites of the Cérdigo Fm. This emersive event could have had a minor impact on the carbon isotope signal, likely mildly affecting the last few metres of the tight micritic Sagrado Corazón limestone succession. The duration of the emersive event is calibrated by the record of *D. grandis* group ammonites above the palaeokarst. This means that the emersive horizon occurred within the same ammonite biozonal range (*D. furcata*) with an undefined duration.

4.1.3. Cérdigo Formation

The Cérdigo Fm is a 9-m-thick nodular limestone unit of the Castro Urdiales section (Fig. 3) that may thicken up to 100 m 8 km to the east in the Muskiz area (Rosales, 1995). The Cérdigo Fm bioclastic calcarenites with corals and ostreids are overlain by marlstones and black lutites of the El Haya Fm (Rosales, 1995; Rosales et al., 1994). The Cérdigo Fm consists mainly of wavy calcarenites and silty marlstones with ostreids, glauconite and ammonites (metres 227 to 236 of figure 2) that were deposited in an open marine environment at slightly deeper-water with respect to the underlying Sagrado Corazón limestones. Based on the sedimentological attributes and the observed lateral facies transitions in other areas of the BCB, the range of estimated depth is 15/50 m (e.g., García-Mondéjar and Fernández-Mendiola, 1993). A prominent glauconitic interval comprising sand-sized glauconite grains extends from metre 231 to 234. In the initial report of Rosales (1995), the boundary between Cérdigo and El Haya Fms was diachronous and the latter exhibited a 3-m-thick glauconitic siltstone marker-level which contained *Deshayesites* sp., *Dufrenoyia* sp., *Dufrenoyia lurensis*, *Cheloniceras (Epicheloniceras) volgense*, *Cheloniceras (Epicheloniceras)* sp. juv. and *Aconeceras* cf. *nisus* (Rosales, 1995) (Figs. 3, 4). We here demonstrate that this glauconite level occurs within the Cérdigo Fm and not in the El Haya Fm as previously reported. Additionally, a distinct hardground is recognised at metre 228.

The originally recovered ammonites suggested a condensed interval including both lower and upper Aptian specimens (Rosales, 1995). Rosales et al. (1994) attributed an upper Aptian age to the Cérdigo Fm. This interpretation is modified after the analysis of newly collected specimens, together with the revision of the earlier ammonite finds, providing an improved stratigraphic framework (Fig. 3). The recently found ammonites include *Cheloniceras* sp., *Deshayesites* sp., *Sinzovia* sp., *Deshayesites* sp. *grandis* group and *Cheloniceras* cf. *mackesoni* (Fig. 3). This association would traditionally be assigned to the *deshayesi* Zone of the lower Aptian. Nevertheless, a broader perspective of the Basque-Cantabrian stratigraphic framework favours a different interpretation. There is strong evidence that the Sarastarri, Peñascal and Sagrado Corazón limestone units form part of a generalised carbonate platform episode of near isochronous character within the *furcata* Zone (Fig. 5). This correlation is consistently supported by an extensive collection of ammonite associations, carefully identified by Aptian taxonomic specialist H. G. Owen (Fernández-Mendiola et al., 2018; García-Mondéjar et al., 2009, 2015a,b, 2019; Millán et al., 2009).

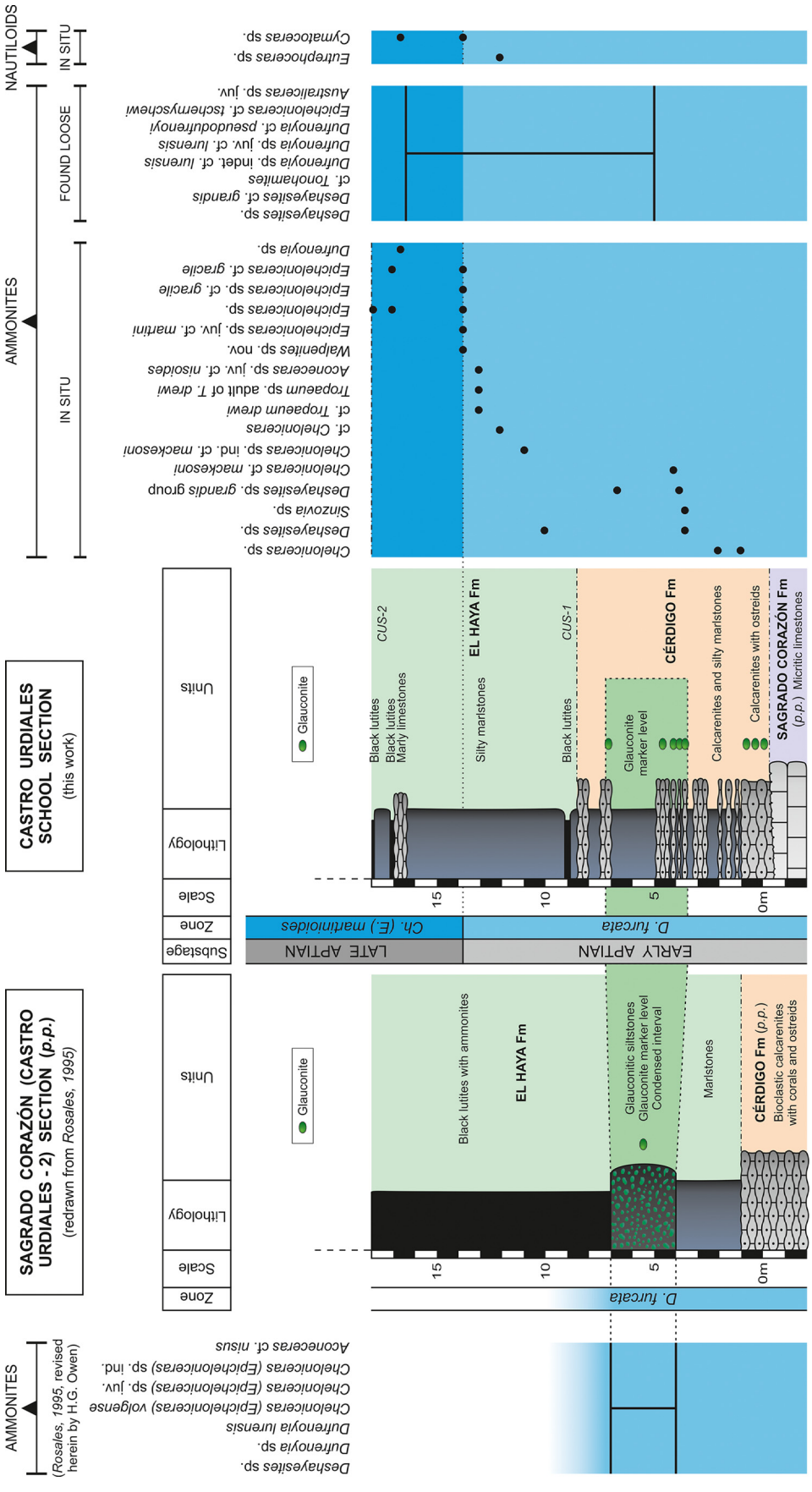

Fig. 3. Updated and detailed stratigraphy of the Castro Urdiales School section, by comparison with the preexisting Sagrado Corazón (Castro Urdiales-2) section. The Castro Urdiales School section encompasses the top of Sagrado Corazón Fm, the Cérdigo Fm and the base of El Haya Fm. Lithofacies and ammonite/nautiloid occurrences are highlighted. Note the presence of the glauconite marker level in the Cérdigo Fm and two black lutite horizons (CUS-1 and CUS-2) in the El Haya Fm.

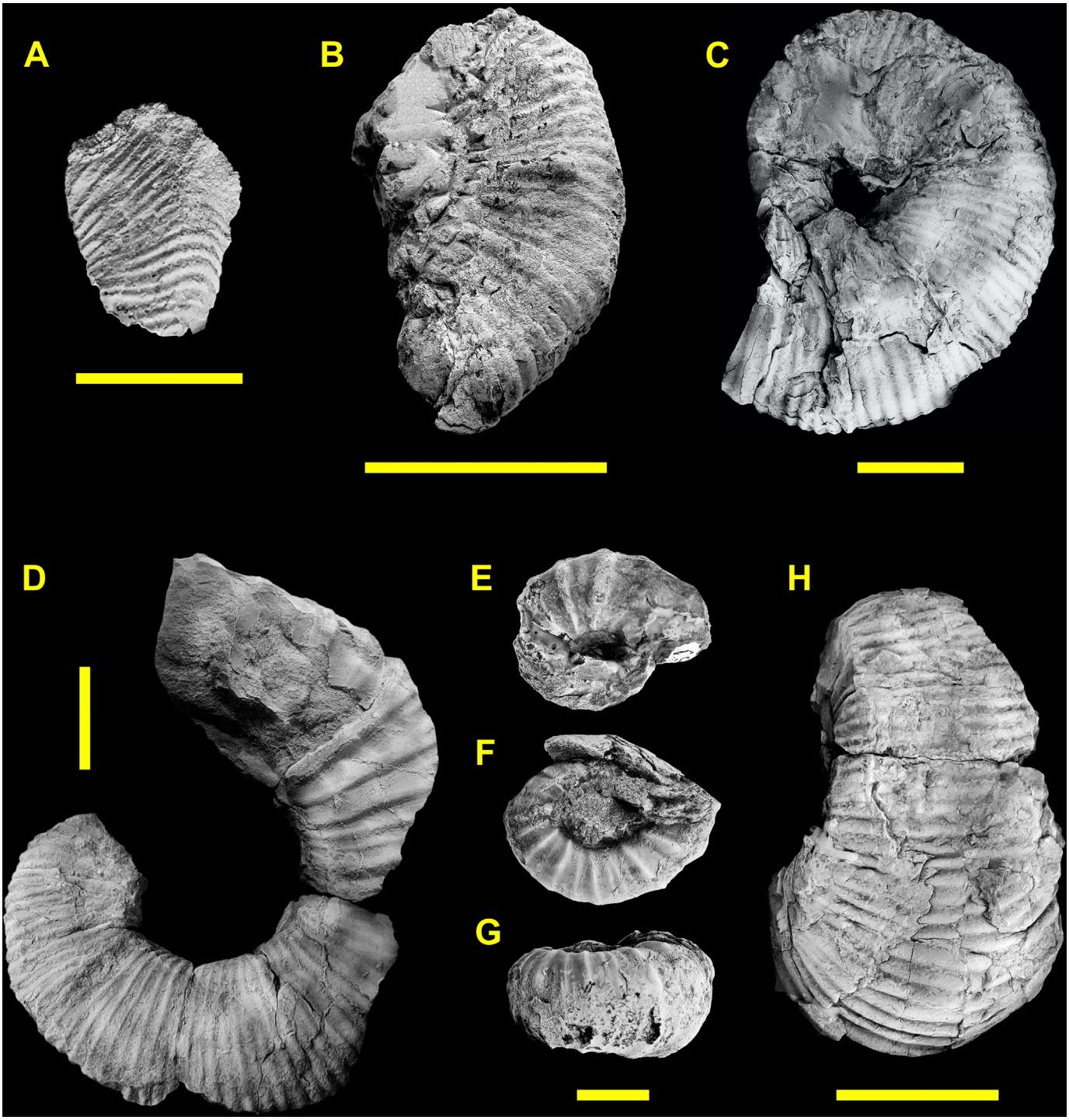

Fig. 4. Aptian ammonites from the Castro Urdiales School section. A) *Deshayesites* sp. juv., CS-R-21. B) *Cheloniceras* cf. *mackesoni*, Cérdigo Fm, CS-10B. C) cf. *Tropaeum drewi* Casey, El Haya Fm, CS-30-1. D) *Tropaeum* sp. adult of *T. drewi* Casey, El Haya Fm, CS-30-2. E) *Epicheloniceras* sp., El Haya Fm, CS-30-12. F-G) *Epicheloniceras* sp. juv., El Haya Fm, CS-30-19. H) *Epicheloniceras* cf. *gracile* Casey, El Haya Fm, CS-36-1. The scale bar is 1 cm long in A, E, F and G, and 5 cm long in B, C, D and H.

Based on these assumptions, the Cérdigo Fm is placed in the *furcata* Zone. This interpretation is additionally supported by the following evidence: 1) *Cheloniceras meyendorfi* (a marker of the *bowerbanki/furcata* Zones, is located at the base of the carbonate platform limestones of Peñascal Fm (Fernández-Mendiola et al., 2018; Fig. 5), and 2) *Palorbitolina lenticularis* and *Iraqia simplex* are found in limestones above the Lareo Fm of the Aralar Mountains, which indicate a lower Aptian age.

4.1.4. El Haya Formation

The El Haya marlstones overlie the wavy calcarenites of Cérdigo Fm (Fig. 2). The thickness of the type section in El Haya (7 km east of Castro Urdiales) is 200 m, progressively decreasing westwards and increasing towards the depocenter of Bilbao. The reported age of the El Haya Fm is upper Aptian extending up to the *jacobi* Zone (Rosales, 1995). We will deal just with the basal part of the unit that contains abundant ammonites, ostreids, belemnites and nautiloids

indicative of more distal environments than the underlying Cérdigo Fm, ranging from slope to intraplatform basin settings. Two organic-carbon-rich black-lutite horizons (CUS-1 and CUS-2) are interspersed in silty marlstones at metres 9 and 17/18 of the Castro Urdiales School section, respectively (Figs. 2, 3). CUS-1 is 30 cm thick and reaches TOC contents of 1.69 %wt, whereas CUS-2 Level is composed of two distinct dark-coloured layers: a first 20-cm-thick black-lutite bed is overlain by 75 cm of silty marlstones, which in turn is succeeded by a 10-cm-thick level reaching 1.02 % wt TOC. Both CUS-1 and CUS-2 levels exhibit fissility and lack bioturbation. Laminated CUS beds suggest deposition in highly dysoxic or anoxic environments based on sedimentological fabrics. The absence of infauna and meiofaunal grazers are interpreted as oxygen deficient environments according to Arthur and Sageman (1994) classification of oxygen levels in palaeoenvironments.

The lowermost ammonite association (metres 7.2 to 13.8 of figure 3) comprises *Deshayesites* sp., *Cheloniceras* sp. ind. cf. *mackesoni*, *Tropaeum drewi* and *Aconeceras* sp. juv. cf. *nisoides* (Fig. 4). Together they indicate the lower Aptian *Dufrenoyia furcata* Zone. The second part of the lower El Haya Fm (metres 13.8 to 18 of figure 3) yields the following ammonite fauna: *Epicheloniceras* sp. juv., *Epicheloniceras* sp. juv. cf. *martini*, *Epicheloniceras* cf. *gracile*, *Walpenites* sp. nov. and *Dufrenoyia* sp. (Fig. 4). This association suggests the upper Aptian lower *Epicheloniceras martini* Zone (equivalent to the *Ch.* (*E.*) *martinioides* Zone of Casey, 1961). Ammonite specimens that were found loose include *Deshayesites* cf. *grandis*, cf. *Tonohamites*, *Dufrenoyia* sp. juv. cf. *lurensis*, *Dufrenoyia* cf. *pseudodufrenoyi*, *Epicheloniceras* cf. *tschernyschewi* and *Australiceras* sp. juv. They are shown in figure 3 as a complementary association, bracketing the likely provenance interval which spans from the middle part of the Cérdigo Fm to the basal El Haya Fm.

4.2. Geochemistry

4.2.1. Carbon isotope stratigraphy

The $\delta^{13}C$ results are plotted in figure 2 for both inorganic and organic fractions (see table in supplementary material section). The $\delta^{13}C_{carb}$ curve displays a lower segment (from metre 0 to 20) that reveals a rising trend in the isotopic values from +4 to +5‰. Then the curve stabilises and values stand over +5‰ along a large part of the limestone succession (metres 20 to 180), locally reaching near +6‰. The final tendency in the Sagrado Corazón Fm is a descending line to values of +2‰ (metres 180 to 227). Here there is a zigzagging segment followed by a sharp negative trend from +2 to −1‰ up to the top of the section.

The $\delta^{13}C_{org}$ curve for the organic fraction shows a general shape that mimics that of the inorganic fraction equivalent (Fig. 2). Values in the lower orbitolinid segment up to metre 13 range around −25‰. Then the values rise throughout the Sagrado Corazón Fm staying around −21‰. In the upper part of the limestones there is a pronounced zigzagging trend from metre 200 to the top of the unit. The transition to the Cérdigo Fm is accompanied by a drop of isotope values down to −24‰. The final segment of the curve records a lowering down to −27‰ in the El Haya Fm.

In summary, there is a $\delta^{13}C$ positive trend with maintained maximum values for most of the Sagrado Corazón limestones and a $\delta^{13}C$ negative excursion onset at the base of the Cérdigo Fm. The Basque-Cantabrian basinwide extension of this positive trend is discussed below. These geochemical curve patterns within an accurate biostratigraphic framework can be used in basinal and worldwide correlations.

4.2.2. Total organic carbon (TOC)

The TOC contents reveal very low concentrations of organic matter in the Sagrado Corazón limestones (Fig. 2, metres 2 to 227 of the section). Thereafter, from metre 227 to 245, TOC values increase throughout the silty marlstones and black lutites of Cérdigo and El Haya formations. There are two significant intervals where TOC content exceeds 1%. These maxima are reached at metres 237 and 245 of figure 2 (respectively), just at the base of El Haya Fm. These organic-matter-enriched horizons encompass black-lutite layers, and they are herewith referred to as CUS-1 and CUS-2 levels (see metres 9 and 17/18 of figure 3). CUS-1 lies in the early Aptian *Dufrenoyia furcata* Zone, whereas CUS-2 belongs to the late Aptian *Ch.* (*E.*) *martinioides* Zone.

5. Discussion

In this chapter, the significance of new findings on the stratigraphy of the Aptian of Castro Urdiales and their basinwide correlation are highlighted (Fig. 5), and its relationship with Aptian oceanic anoxic events is discussed. Biostratigraphic and chronostratigraphic aspects of anoxic events are first considered, followed by examination of environmental aspects during deposition of anoxic/dysoxic facies associations.

5.1. Chemo-biostratigraphic correlation

Chemostratigraphic and biostratigraphic data are combined to attempt intrabasinal and extrabasinal correlation of the Aptian stratigraphy of the BCB with the well-known reference section of the Vocontian Basin in southeastern France (Herrle et al., 2004, 2010) (Fig. 5). Examination of the correlation chart of figure 5 reveals complex stratal packages with multiple lateral facies variations. Within this framework, carbon isotope excursions and organic-carbon-rich biostratigraphically calibrated horizons are addressed below.

5.1.1. Furcata positive CIE

A reference marker in the stratigraphic chart of figure 5 is a widespread limestone episode extending throughout the BCB. Namely, the lower Aptian Sagrado Corazón limestones correlate with the coeval Peñascal limestones of the *Dufrenoyia furcata* Zone, based on regional correlation and mapping (Fernández-Mendiola et al., 2018). An additional robust marker horizon is the major worldwide positive excursion of $\delta^{13}C$ immediately postdating OAE 1a, with values exceeding +4 to over +5‰. This episode of persisting high carbon isotopic values is unique throughout the Phanerozoic record and represents the maximum positive CIE of the Early Cretaceous. They correspond to C7 interval of Menegatti et al. (1998) and are interpreted as the result of enhanced global light carbon burial and are documented from sections worldwide (e.g., Bottini et al., 2015; Castro et al., 2021). Based on the planktonic foraminiferal biozones in the reference section of Cismon core (NE Italy), C7 spans mostly to the *Leupoldina cabri* Zone and its uppermost part falls within the *Globigerinelloides ferreolensis* Zone (Erba et al., 1999). The overall high $\delta^{13}C$ values of C7 show minor internal negative shifts and oscillations (e.g., Núñez-Useche et al., 2014). These variations have allowed some authors to subdivide segment C7 into discrete sub-segments or zones (e.g., Herrle et al., 2004).

In the BCB, C7 isotopic interval is traceable from the Sarastarri Fm of the Igaratza section (Aralar Mountains) to the Peñascal Fm of the Mount Pagasarri section, as well as to the Castro Urdiales School section (Fig. 5). A similar positive excursion has been identified in the Serre Chaitieu section (Herrle et al., 2004) within a series of alternating marlstones, calcareous marlstones and lutites corresponding to the green-coloured band of figure 5.

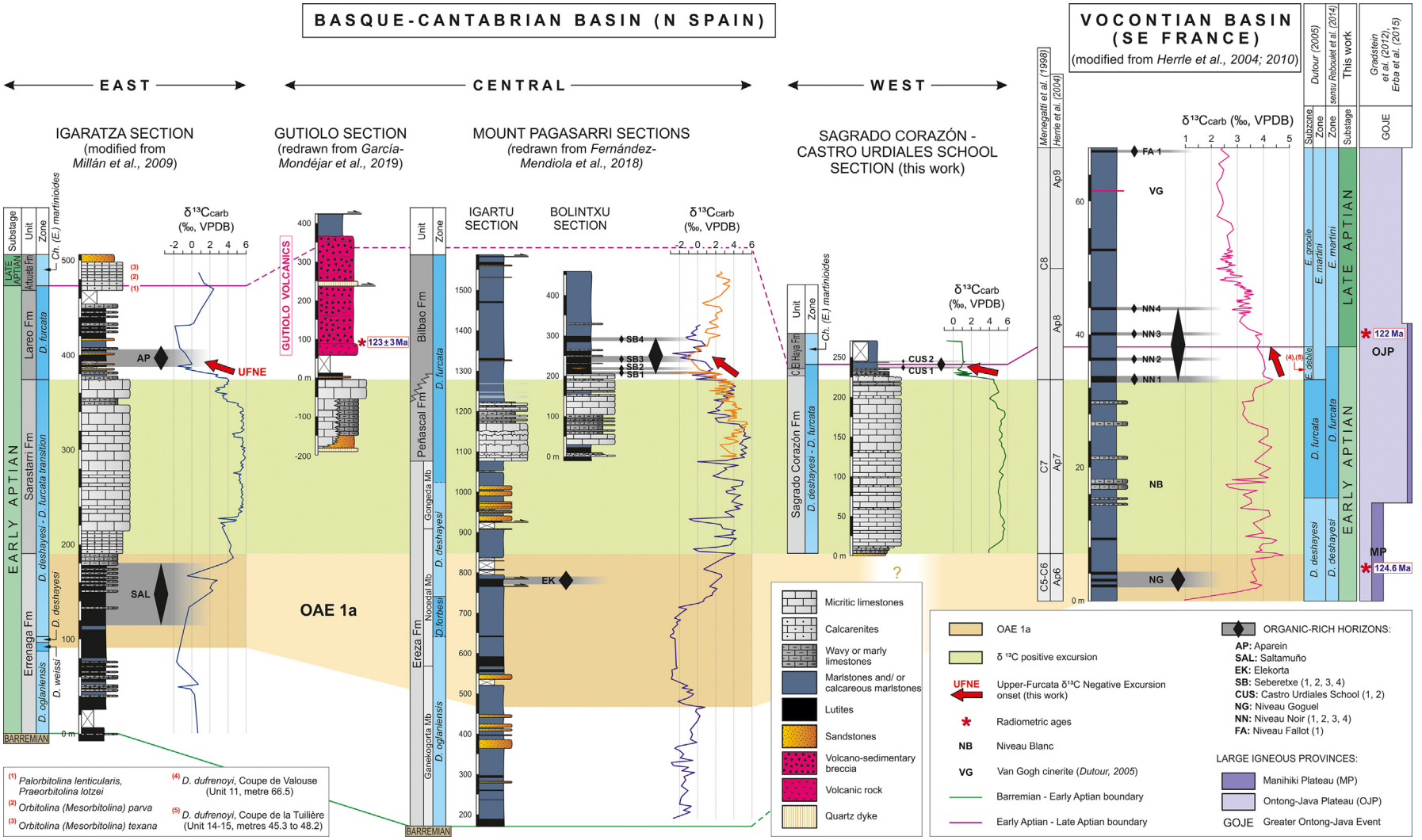

Fig. 5. Geochemical correlation among three sections in the BCB (Igaratza, Bilbao and Castro Urdiales) and the Vocontian Basin (SE France). In all sections $^{13}\delta C_{carb}$ data show a lower negative excursion (OAE 1a), an intermediate positive excursion with the highest absolute values reached in the Cretaceous (close to +6‰, see also Gradstein et al., 2004, their Figure 19.3), and the sharp start of an upper negative excursion at the end of the early Aptian. This last excursion begins with a palaeogeographical change from limestone-rich successions to dark, marly-rich units. It also begins with a TOC enrichment that corresponds to the Aparein Level in the BCB and the first Niveaux Noirs of the Vocontian Basin. NN1 and NN2 correspond to the uppermost lower Aptian instead of the basal upper Aptian of Herrle et al. (2004), because the earliest appearance of the ammonite genus *Epicheloniceras* occurs with coeval *Dufrenoyia dufrenoyi* ammonite (see Dutour, 2005). The Gutiolo section near Bilbao shows volcanic rocks almost from the base of the negative CIE of UFNE, related to the opening of Bay of Biscay (García-Mondéjar et al., 2019). We consider this volcanism the immediate cause of the palaeogeographic and geochemical changes at the early-late Aptian transition. Additional key fossils of biostratigraphic significance: (1), (2) and (3) from Millán et al. (2014); (4) and (5) from Dutour (2005).

5.1.2. Upper Furcata negative CIE

In Castro Urdiales, C7 segment is followed by a significant $\delta^{13}C$ negative excursion close to the early-late Aptian transition. The red arrow in figure 5 marks the Upper Furcata Negative Excursion (UFNE). UFNE is also present in the Igaratza section (Aralar Mountains) and Mount Pagasarri section (Bilbao area), and reevaluation of existing datasets allows the identification of UFNE in the Vocontian Basin (France) (Fig. 5). Here, above the C7, a significant $\delta^{13}C$ negative excursion is recognised as earliest late Aptian by Herrle et al. (2004, 2010).

Nevertheless, ammonites reported in La Tuilière section (Dutour, 2005) reveal even an earlier age. In fact, *Dufrenoyia* and *Epicheloniceras* genuses coexist in unit 14/15 (metres 45.3–48.2 m). The full association of this interval includes: *Dufrenoyia dufrenoyi, Pseudohaploceras angladei, Zuercherella zuercheri, Colombiceras crassicostatum, Epicheloniceras martini, Epicheloniceras eotypicum and Salfeldiella (G.) paquieri*. Additionally, in the Valouse section of SE France, *Dufrenoyia dufrenoyi* is also interspersed with *Epicheloniceras* specimens and is ascribed to the *martini* Zone (unit 11, 66.5 m; Dutour, 2005) (Fig. 5). According to the general consensus among the Cretaceous ammonite specialists, *Dufrenoyia dufrenoyi* is indicative of a late early Aptian age, whereas *Epicheloniceras* sp. is characteristic of the late Aptian (Reboulet et al., 2014). But in the Vocontian sections both taxa coincide partly in the same stratigraphic intervals. It has been suggested that the last occurrence of *Dufrenoyia dufrenoyi* should be considered the top of the *furcata* Zone (Reboulet et al., 2014).

Based on this assumption, the latest early Aptian would be represented in beds originally defined as basal Ap8 stratigraphic interval (Herrle et al., 2004). These beds represent the UFNE (Fig. 5) and are overlain by a further sustained negative CIE that extends across intervals Ap8 to Ap10 from the *Ch. (E.) martiniodes* ammonite Zone and *G. ferreolensis* to *G. algeriana* planktonic foraminifera Zones (Herrle et al., 2004). In figure 5, in the Serre Chaitieu section the red arrow representing UFNE is followed, from 38 to 64 m, by a sustained negative CIE that encompasses Ap8 and half of Ap9 Zones of Herrle et al. (2004).

The upper lower Aptian UFNE is also tentatively correlated at a superregional scale based on available stratigraphic records. A negative CIE is recorded in the Cismon section encompassing the basal *G. ferreolensis* Zone (base of C8 segment of Menegatti et al., 1998). This has traditionally been considered as basal upper Aptian. However, in-depth biostratigraphic analysis in the La Tuilière section (France) has revealed transitional forms of *Praehedhergella luterbacheri*, an ancestor form of *G. ferreolensis* (Moullade et al., 2008). *P. luterbacheri* appears in beds containing *Dufrenoyia* sp., with distinct lower Aptian affinity. The occurrence of *P. luterbacheri* in the *furcata* Zone is also supported by evidence from Crimea (Brovina, 2017). Therefore, in the condensed section of Cismon, the negative CIE overlying C7 could partly represent the UFNE. Similarly, in the Cau section of the Betic Cordillera (SE Spain), a negative CIE is reported in the uppermost part of the *furcata* Zone. Supporting this view, the D. *furcata* ammonite Zone is made partly coeval to the basal *G. ferreolensis* Zone (above metre 29, segment C8 in figure 3 of Moreno-Bedmar et al., 2012).

Elsewhere, in the Isle of Wight (UK), the negative CIE also falls in the *T. bowerbanki* Zone (from metre 130 to 150 in figure 1 of Gröcke et al., 1999), A similar negative CIE occurs in marlstones of the Cassis – La Bedoule section (SE France) in a very condensed *furcata* Zone interval (above metre 120, in figure 4 of Moullade and Tronchetti, 2010), or in the updated Gare de Cassis/La Marcouline Quarry/Camping section with a marked negative CIE in the upper Bedoulian (lower Aptian) (m 120, C8 interval in figure 2 of Kuhnt et al., 2011). These negative CIEs could be considered as expressions of UFNE.

5.1.3. CUS 1–2, Aparein and Niveau Noir levels

Stratigraphic correlation across the BCB highlights the synchronicity between the organic-carbon-rich Aparein Level of the Aralar Mountains and CUS-1 Level of Castro Urdiales, whereas CUS-2 Level lies above this correlation line (Fig. 5). An attempt to correlate the Aparein Level with likely equivalents of SE France is summarised below. Four Niveau Noir intervals are recognised in the Vocontian Basin (NN1 to NN4, Fig. 5), which occur immediately above the C7 segment of the *D. furcata* Zone. According to ammonite extent reevaluation based on Dutour (2005), NN1 and NN2 fall within the early Aptian and are synchronous with the UFNE. These horizons are also coeval with the black lutites of Aparein Level of the Aralar Mountains, the Seberetxe black lutites of Mount Pagasarri and the first black-lutite bed of Castro Urdiales (CUS-1, Fig. 5). Ammonites found in the basal 300 m of the marly Bilbao Formation (Mount Pagasarri), which are laterally equivalent of the Cérdigo Fm and basal El Haya Fm (Fig. 5), reveal lower Aptian *Dufrenoyia*-dominated associations, and are coetaneous with the Gutiolo volcanics based on lithostratigraphic correlation and facies mapping along a 4 km transect (Fernández-Mendiola et al., 2018). Our results indicate that the black-shale horizon CUS-2 of Castro Urdiales can be correlated with NN3 and NN4 of the Vocontian Basin at the *Epicheloniceras martini* Zone of the lowermost upper Aptian. Slightly above these black-shale horizons a bentonitic volcanic tuff bed is recorded in the *E. martini* Zone. This volcanic deposit, known as Van Gogh layer (Bréhéret, 1997), could be time-equivalent to CUS-2 of the Castro Urdiales section and also to the topmost Gutiolo volcanic deposits of the BCB (Fig. 5).

Recent published results (Frau, 2021a,b) contradict the original viewpoint of a late early Aptian age of Aparein (Fernández-Mendiola et al., 2018; García-Mondéjar et al., 2009; Millán et al., 2009) and place the age of the Aparein Level of the Aralar Mountains in the early late Aptian. C. Frau arguments for the age reassignment are based on: 1) the analogies between the carbon isotope curve trends in both the BCB and the Vocontian Basin, and 2) the reidentification of two ammonite specimens from photographic plates published by other authors, without *in situ* examination of specimens from the collections stored at the University of the Basque Country. Our correlation summarised in Figure 5 supports the original hypothesis that Aparein Level is lower Aptian (Fernández-Mendiola et al., 2021). The strength in the stratigraphic framework comes from the biostratigraphic record coupled with carbon isotope stratigraphy extended and correlated throughout the BCB, and contradicts the viewpoint of C. Frau. In Frau (2021a,b), the negative CIE (UFNE) of ammonite-bearing Aparein Level from the *furcata* Zone is wrongly correlated with ammonite-bearing Fallot beds from the upper Aptian *martini* Zone of the Vocontian Basin. In summary, the evidence suggests that there is no age equivalence between the segments of the correlated negative CIE suggested in Frau (2021a,b).

5.1.4. Wezel and Aparein black-shale levels

The recently published Wezel Level (Matsumoto et al., 2021) is tested as likely synchronous interval to the Aparein Level. The Italian Aptian (Umbria/Marche Basin) records episodic black shales linked to the massive volcanic eruptions of the Pacific Ocean. Monitoring of the submarine eruptions using Osmium isotopic compositions enables recognition of two close episodes of anoxia in the early Aptian: the Selli Level associated with OAE 1a and the overlying Wezel Level.

The analysis of stratigraphy, as well as of carbon and oxygen isotope data, reveal that the black-shale Wezel Level is included in the *Leupoldina cabri* Zone and that it lies in the middle of Ap7 (Matsumoto et al., 2021, figure 2, metre 3). The Ap7 and lower half Ap8 interval (see their figure 2, from metre 2 to metre 5) reveal

persistent $\delta^{13}C$ values above +4 and 4.5‰ within the uppermost *L. cabri* and *G. ferreolensis* Zones. According to the reference curve of Menegatti et al. (1998), $\delta^{13}C$ values above +4 and 4.5‰ belong to the C7 positive excursion (Scholle and Arthur, 1980; Weissert and Erba, 2004; Weissert and Lini, 1991; Weissert et al., 1998). Based on this evidence, C7 positive excursion encloses the Wezel Level in the Umbria-Marche Basin. High values of $\delta^{13}C$ extend throughout the lower half of Ap8 up to the top of *G. ferreolensis* Zone. This Taxon Range Zone was originally attributed to the late Aptian (e.g., Coccioni et al., 2007; Ogg et al., 2016). However, recent investigations in the Chaqiela section of Tibet expand this attribution and propose that *G. ferreolensis* spans from the lower to the upper Aptian (Fang et al., 2021). We favour that the Wezel Level is a likely equivalent of the black shale of Chaqiela section.

Close comparison of the Wezel and Aparein enveloping carbon isotopic signals reveal a lack of fitting trend. This suggests that they could be different events. The Wezel Level lies in Ap7 interval, a segment of the carbon isotope curve that is adscribable to C7 segment of Menegatti et al. (1998). On the other hand, the Aparein Level and its equivalent CUS-1 Level in Castro Urdiales, occur in the negative CIE immediately succeeding C7 interval of Menegatti et al. (1998). Additional future work in basins worldwide could help clarify and reveal controlling processes involved in this geologic period of time.

5.1.5. Biostratigraphic constraints

Constraining factors to establish the stratigraphic position of the organic-carbon-rich levels around OAE 1a have been acknowledged including 1) insufficient calibration of Aptian micropaleontological and ammonite datums and 2) improper deciphering of isotopic signatures (Moullade et al., 1998). Biostratigraphic and chemostratigraphic calibration and accurate correlation is essential to a successful research outcome.

The biostratigraphy of OAE 1a and overlying related anoxic episodes in the BCB is exposed below. The worldwide biostratigraphic range of OAE 1a differs among authors (e.g., Moreno-Bedmar et al., 2009). In the BCB this event includes the Elekorta and Saltamuño levels (Fig. 5) as evidenced by ammonites, benthic foraminifera (mainly orbitolinids) and chemostratigraphy. According to this dataset, OAE 1a ranges from the *D. oglanlensis* Zone (pars) to the *D. deshayesi* Zone (pars) (Fernández-Mendiola et al., 2018; García-Mondéjar et al., 2009, 2015).

The biostratigraphy of the lower Aptian organic-rich CUS-1 Level (El Haya Formation, Fig. 5) is consistent with coeval ammonite and benthic foraminiferal associations reported in laterally equivalent strata of the BCB, such as: 1) the Lareo Fm of the Aralar Mountains (García-Mondéjar et al., 2009), which includes coexisting and/or interspersed *Deshayesites* and *Dufrenoyia* specimens. Namely, scientific evidence published as photographed specimens include: *Aconeceras* cf. *nisoides*, *Aconeceras* cf. *haugi*, *Cheloniceras* (*Cheloniceras*) sp., *Deshayesites* cf. *deshayesi* (García-Mondéjar et al., 2009, Fig. 6), and *Dufrenoyia* cf. *lurensis* (García-Mondéjar et al., 2009, Fig. 7), 2) the Bilbao Fm of Mount Pagasarri with *Tropaeum* cf. *benstedi* and *Tropaeum drewi* (Fernández-Mendiola et al., 2018) and 3) the Robayera Fm of the western BCB (Fernández-Mendiola et al., 2015).

The classical lower Aptian sedimentary successions exhibit dominant deshayesitids of the *deshayesi* Zone overlain by dufrenoyids and *Tropaeum* of the *furcata* Zone, which in turn are succeeded by epicheloniceratids of upper Aptian affinity (e.g., Reboulet et al., 2014). In Egypt, *Dufrenoyia dufrenoyi* and *Epicheloniceras waageni* occur in a condensed bed (Abu-Zied, 2008). Similarly, the above-mentioned BCB localities show atypical ammonite associations that can be explained either by 1) inaccurate biostratigraphic constraints in BCB and/or 2) differences in stratigraphic completeness of the rock record among diverse basins.

The biostratigraphic foundation for the correlation diagram of figure 5 derives from the scientific examination of over 300 ammonite specimens of the lower Aptian of the BCB. Careful comparisons with the Natural History Museum collections in London, based on long-term expertise (H. G. Owen) have served as reference in order to decipher taxonomic attributes of the faunas. Additional challenges come from the sometimes incomplete or deformed specimens. Profound expertise of the characteristic taxonomic parameters to discern among taxa is required. An individual specimen could perhaps be incorrectly determined due to the plasticity of the ammonite evolutionary scheme, but whole associations are conclusive for the biostratigraphic assignments. The results of the analysis of the whole association and comparison with equivalent type collections point to a widespread development of a lower Aptian marlstone/lutite sedimentary wedge overlying the *furcata* carbonate platform in the BCB (Fig. 5). The thickness of this wedge ranges from 9 m in low subsident areas of the Basin like Castro Urdiales, to more than 300 m in the highly subsident Bilbao area, and to over 100 m in the Aralar Mountains of the BCB (Fig. 5).

5.1.6. Lower Aptian sedimentary thickness

When comparing faunal associations from different basins it is important to bear in mind the rates of sedimentation and thickness of the rock record. If we compare the average thickness of the lower Aptian between the BCB (475 m for Igaratza; over 1400 m for Mount Pagasarri; 1115 m for Castro Urdiales, based on Rosales, 1995) and the Vocontian Basin (38 m, Fig. 5), we can conclude that the sedimentary record of the BCB is over 12 times thicker in Igaratza, almost 37 times thicker in Mount Pagasarri and ~29 times thicker in Castro Urdiales than in the Vocontian Basin. These relatively lower thicknesses of the lower Aptian are a common feature in numerous sections from other sedimentary basins such as: 138 m in La Bédoule (Kuhnt et al., 2011), 22 m in Cismon (Menegatti et al., 1998), 63 m in the Cau section of SE Spain (Quijano et al., 2012), 52 m in Santa Rosa Canyon-California (Bralower et al., 1999), 15 m in Allsttäte-Germany (Lehmann et al., 2012), and 45 m in the Iberian margin DSDP 398 (Jenkyns, 2018). This evidence suggests that the comparatively thicker series of the BCB could have explained a more complete preservation of some of the ammonite evolutionary steps, unrecorded in less subsident and/or more condensed successions. For instance, an unusual Lazarus effect of *Deshayesites*, *Dufrenoyia* and *Epicheloniceras* is recognised in several sections of the BCB. In the Aralar Mountains, *Deshayesites* specimens of the Errenaga Fm are replaced by a level containing *Dufrenoyia* in the younger Lareo Fm, but higher up in this unit *Dufrenoyia* disappear and *Deshayesites* become abundant up to the top of the lower Aptian succession (García-Mondéjar et al., 2009). Moreover, at the base of the Bilbao Fm of Mount Pagasarri section, *Epicheloniceras*, a representative of the upper Aptian, appears on top of the Peñascal limestones in the same horizon with *Dufrenoyia* and *Deshayesites*. Upwards, *Epicheloniceras* is further overlain by 300 m of alternating beds containing *Tropaeum*, followed by *Deshayesites* and *Dufrenoyia* co-occurring taxa (Fernández-Mendiola et al., 2018). This is at odds with current palaeontological accepted view.

In summary, a genus apparently disappears for short periods from the fossil record, and is succeeded by a new genus, but the former genus reappears later in a Lazarus taxa-like pattern. These could be observational sampling artifacts as the fossil record is inherently sporadic and only a very small amount fraction of organisms become fossilised and preserved, and even a smaller fraction is discovered before destruction. These issues together

with differential rates of subsidence should be taken into consideration when comparing sedimentary basins aside.

5.1.7. Radiometric ages of lower Aptian OAEs

The absolute age duration of the Aptian remains a topic of discussion (Fiet et al., 2006; Gradstein et al., 1994, 2004, 2012; Huang et al., 2010). Radiometric dating of OAE 1a is poorly constrained, and reports vary from 120 to 124.55 Ma (e.g., Huang et al., 2010; Li et al., 2008). In the BCB, there is a radiometric age for the volcanics of the Gutiolo section, which are located east of Castro Urdiales lying above C7 interval and interfingering with the Aparein Level (Fig. 5). The age of the Gutiolo volcanics is 123 ± 3 Ma (García-Mondéjar et al., 2019). This fits with values outlined in the Ontong Java Plateau: 124.6 Ma by Timm et al. (2011) and 122 Ma (Chambers et al., 2004; Erba et al., 2015; Gradstein et al., 2012) (Fig. 5). In the same way, volcanic rocks in Lebanon very likely belong to the same event with ages ranging between 125 and 123 Ma (Garfunkel and Katz, 1967; Itamar and Steinitz, 1988; Lang and Steinitz, 1994; Lang et al., 1988).

However, the absolute dating of the Gutiolo volcanics does not fit into the most recently published geochronological charts (Olierook et al., 2019; Zhang et al., 2021). The age of the Barremian-Aptian boundary has been corrected in the Geological Time Scale – GTS 2012 to the more recent 2020 version. The earlier estimated age was 126.3 ± 0.4 Ma (Gradstein et al., 2012), whereas the current International Commission on Stratigraphy chart indicates an approximate age of 125 Ma (Cohen et al., 2013), and the new GTS-2020 places the base of the Aptian at 120.8 Ma. The geochronological recent updating is based on new selected radioisotopic dates since 2012 in Svalbard archipelago (Artic Ocean). Nevertheless, revision of the selected radioisotopic dates published since 2012 do not reveal a systematic offset to younger ages in the early Aptian (Zhang et al., 2021, their Fig. 1). On the other hand, the new lower boundary of the Aptian derives from zircons sampled from a lower Barremian bentonite layer in Svalbard, with a 123.1 ± 0.3 Ma age (Midtkandal et al., 2016). The bentonite is located 40 m below OAE 1a, and the authors stated that they could not accurately determine the Barremian-Aptian boundary. These authors performed the sampling of zircon grains by visual hand-picking. Several studies have highlighted the need to quantify methodological limitations in detrital zircon geochronology datasets to allow robust interpretations (e.g., Dröllner et al., 2021; Ibañez-Mejia et al., 2018). These studies reveal evidence of preferential selection bias (based on grain shape and colour) induced during handpicking throughout the sampling procedure. Consequently, a significant methodological pitfall is determined concerning the use of relative age peaks in detrital zircon U–Pb geochronology. These technical issues could have influenced the accuracy of the dates and the tephra chronological divergence in radioisotopic dates.

On the other hand, the Aptian palaeoenvironments in Svalbard were influenced by mantle plume activity formed by a number of LIPs such as the Ontong Java Plateau and the High Artic Large Igneous Province (HALIP, Midtkandal et al., 2016). Interestingly, the age of the HALIP suggests a peak activity around 124–125 Ma, and the ages obtained in sills from Franz Josef Land archipelago are 123 Ma (Corfu et al., 2013). These values fall within the age range reported in the Gutiolo volcanics of the BCB in the vicinity of Castro Urdiales. Additionally, HALIP-related volcanic sill emplacement could have released significant amounts of CO_2 to the atmosphere and contributed to the OAE 1a (Polteau et al., 2016). A causal link between rapid climatic changes and LIP activity, where degassing of intrusives is the triggering mechanism is suggested by Ganino and Arndt (2009) and Svensen et al. (2015). This is in accordance with the work of Naafs et al. (2016) demonstrating a doubling of atmospheric CO_2 concentrations during the initial stage of OAE 1a.

5.2. Palaeoenvironmental implications

We will examine the interrelation of anoxic events and carbonate environments and the influence of environmental constraints in the sedimentation of organic-carbon-rich horizons and associated facies.

5.2.1. Organic-rich horizons and carbonate environments

The Sagrado Corazón limestones of Castro Urdiales form part of an isochronous carbonate platform development in the lower Aptian *furcata* Zone of the BCB (Fig. 5). OAE 1a occurs below the platform whereas the Aparein Level overlies it (Fernández-Mendiola et al., 2018; García-Mondéjar et al., 2009, 2015a,b). The Sagrado Corazón shallow-water rudist and miliolid limestones, typifying inner platform environments, were succeeded by slightly deeper-water coral-rudist facies. This platform succession culminated in subaerial exposure and karstification. The end of the carbonate platform sedimentation was linked to active synsedimentary tectonic movements related to the opening of the Bay of Biscay (García-Mondéjar et al., 2004). The carbonate platform was subsequently covered by open-marine ammonite-bearing facies representing a progressive drowning sequence (Cérdigo and El Haya Fms) that includes CUS-1 and CUS-2 organic-carbon-rich levels.

These data suggest that during the formation of the upper Bedoulian Sagrado Corazón limestones, no coeval anoxic event was recorded. On the contrary, evidence from the Castro Urdiales, Bilbao, Igaratza and Cuchía sections reveal that OAE 1a deposits formed during episodes of dominant siliciclastic sedimentation, namely in: 1) the Errenaga Fm of the Aralar Mountains (García-Mondéjar et al., 2009), 2) the Ereza Fm of Bilbao (Fernández-Mendiola et al., 2018) and 3) the Patrocinio Fm of Cuchía (García-Mondéjar et al., 2015a,b; Najarro et al., 2011). Similarly, Aparein, Seberetxe and CUS-1 levels record marly and lutitic sedimentation in intraplatform basinal settings (Fig. 5). Based on this stratigraphic framework, we can infer that in the lower Aptian of the BCB carbonate platform development and anoxia/disoxia are out of phase events.

5.2.2. Ostreids and glauconite

In the BCB there is an upper lower Aptian ostreid-rich interval which forms a marker horizon across a broad area, extending at least from Castro Urdiales and Islares to Bilbao and continuing further eastwards to Gorbea and the Aralar Mountains (e.g., Fernández-Mendiola et al., 2018; García-Mondéjar et al., 2009; Rosales, 1995, 1999). In the Cérdigo Fm of Castro Urdiales, these facies consist of high concentrations of ostreids interspersed with glauconite-rich layers (Figs. 2, 3).

Several studies report the effect of volcanic activity on the origin of glauconite and ostreid mass occurrences. Glauconite origin is often attributed to hydrothermal alteration of volcanic rocks and volcaniclastic material by the active influence of bacteria and chemoorganotrophic microbes (e.g., Reolid and Abad Martínez, 2014). Glauconite usually form under low sedimentation rates and oxic/suboxic conditions with limited terrigenous input often in outershelf/upper slope environments favouring the incorporation of Fe into the grains during early diagenesis (Amorosi, 1995; Odin and Fullagar, 1988; Odin and Matter, 1981). With regards to ostreids, their proliferation is usually associated with favourable feeding sources, as these filter-feeding communities flourish under eutrophic conditions in estuaries and nearshore environments (Toscano et al., 2018). Ostreids also thrive in volcanically-fertilised submarine settings, such as the submarine Tagoro volcano (Canary Islands) erupted in 2011 (Colín-García et al., 2016; González-Vega et al., 2020; Santana-Casiano et al., 2017; Sotomayor-García et al., 2019). Shallow-water hydrothermal systems are an important source of nutrients to the ocean.

Figure 5 illustrates the correlation between the Gutiolo volcano (García-Mondéjar et al., 2019) and adjacent glauconite-and-ostreid facies. We claim that the Gutiolo volcanic activity controlled the chemistry of the surrounding sea-bottom, in such a way that iron releases and volcanic fertilisation of marine waters induced glauconite precipitation and favoured oyster growth. These facies represent a unique episode of exceptional environmental conditions in the BCB and therefore they can be used as a proxy for stratigraphic correlation.

5.2.3. Black shales and volcanism

The lower Aptian was a period of enhanced deposition of organic-carbon-rich facies in oceanic settings, informally known as black shales. This sedimentation might have resulted from several possible factors such as warm oceanic deep waters, reduced current circulation in restricted basins, low dissolved oxygen contents and high marine organic productivity (Arthur et al., 1987; Erbacher et al., 2001; Ryan and Cita, 1977). Dark-coloured and fine-grained organic-carbon-rich facies, including black shales, mudstones and lutites, are a common feature developed in quiet waters and disoxic/anoxic episodes of the Earth's history (Arthur and Sageman, 1994; Arthur and Schlanger, 1979; Schlanger and Jenkyns, 1976). The presence of high amounts of organic matter can be related to productivity and/or anoxia or a combination of both. Punctuated sluggish water circulation in the Cretaceous Atlantic has been proposed as a driver of OAEs (Pedersen and Calvert, 1990). However, sporadic and spatial increases in primary production are needed to account for OAEs (Pedersen and Calvert, 1990).

The timing of black-shale formation has been correlated with eruption of Large Igneous Provinces (LIPs), for example, the OAE 1a with the Ontong Java Plateau (e.g., Ohkouchi et al., 2015). The synchronicity between massive volcanic eruptions and black-shale deposition has been clearly demonstrated based on analyses of lead isotopes ($^{206}Pb/^{204}Pb$, $^{207}Pb/^{204}Pb$, and $^{208}Pb/^{204}Pb$ ratios) and osmium ($^{187}Os/^{188}Os$) recorded in sedimentary successions (Kuroda et al., 2011; Tejada et al., 2009). Volcanism, anoxia and extinctions in the Aptian occurred as a consequence of intense and widespread submarine eruptions in the Pacific region (Vogt, 1989). In this regard, volcanic tuffaceous beds are recognised below and above the black shales of OAE 1a (Marsaglia, 2005). Additionally, elsewhere in the Vocontian Basin, black-shale deposits of the lowermost upper Aptian are punctuated by volcanic cinerite deposits (e.g., the Van Gogh bentonite; Bréhéret, 1997), proving again that active volcanic vents were coeval with dysoxic/anoxic sea-bottoms.

We envisage a similar scenario for the BCB. In fact, the correlation of figure 5 reveals a close match of black-lutite CUS-1 Level of Castro Urdiales with analogous facies of Mount Pagasarri and Igaratza sections (Seberetxe and Aparein levels), which supports contemporaneous formation of high-TOC horizons of the uppermost *furcata* Zone and the Gutiolo volcanics (García-Mondéjar et al., 2019). Deposition of OM in Castro Urdiales occurred in the vicinity of the upper lower Aptian Gutiolo active volcano. The Gutiolo volcanic locus was located 2 km eastwards from the coeval Seberetxe black lutites of Mount Pagasarri sections, 24 km eastwards from anoxic CUS-1 bed of the Castro Urdiales section, and 68 km westwards from the Aparein black shales of the Igaratza section (Fig. 5). Oxygen deficient and nutrient/metal-rich waters were likely expelled from volcanic eruptive sites and associated leaky faults. These waters spread subsequently to more distal areas of the basin. The development of disoxic/anoxic conditions and the subsequent formation of organic-carbon-rich deposits resulted from the activity of submarine hydrothermal vents at the Gutiolo eruptive site and/or at a leaky fault system fed by it.

Our results indicate that the CUS-1 and Aparein levels formed as a consequence of local volcanism but their sedimentation also coincides with LIP volcanism worldwide (Fig. 5). Our contention is that the volcanic activity in the BCB could be an expression of LIP-related volcanic event. They played a major role in the sedimentation of the BCB during intermittent episodes of the early Aptian inducing anoxia, acidification and greenhouse conditions. Extra-basinal time-equivalent candidates for CUS-1 and Aparein levels include: 1) volcanic tuffs of the Mid-Pacific Mountains (DSDP 463, metre 608), with 2% wt TOC peak values, 2) *Australiceras*/*Cheloniceras* ammonite beds of the Fakland Islands (DSDP 551, metre 505), with 4% wt TOC, and 3) facies of metre 1012 of the Angola Basin section, with 6% wt TOC (Bralower et al., 1993).

6. Conclusions

OAE 1a is recorded within shallow-marine open-water siliciclastic units, and is succeeded by a widespread uppermost lower Aptian carbonate platform phase throughout the BCB. In Castro Urdiales there is no record of carbonate platform coeval with OAE 1a. The lower Aptian Sagrado Corazón limestone succession is described with identification of a palaeokarst surface atop. After this episode of subaerial exposure, the Castro Urdiales platform underwent a drowning process in the late early Aptian. This drowning phase encompassed short-lived oxygen deficient periods with black-lutite sedimentation postdating OAE 1a. A first TOC-enriched black-lutite horizon (CUS-1) within the drowned sequence is correlated with the Aparein Level of the *D. furcata* Zone (latest early Aptian), and it is coincident with the inception of a negative $\delta^{13}C$ excursion in the upper *D. furcata* Zone (UFNE), and the NN1 and NN2 levels of the Vocontian Basin. The recognition of the expression of the Aparein anoxic event in more basins around the world needs further testing and could help refine the knowledge of environmental change in the early to late Aptian transition. A second black-lutite layer (CUS-2), which occurs at the base of the late Aptian (*E. martini* Zone), is stratigraphically correlated to Niveau Noirs NN3 and NN4 of the Vocontian Basin. A new ammonite fauna is described, and revision and comparison with former associations help clarify the stratigraphic record. Ammonite dating of basinal facies reveals an early to late Aptian transition.

The Castro Urdiales carbonate platform demise records a period of synsedimentary tectonism that was responsible for both temporary platform emersion and subsequent drowning phase. Block uplift and downlift were linked to a pulse of acceleration in the opening of the Bay of Biscay, during which extensional faults progressively favoured magma ascent to the seafloor. Glauconite-rich deposits and black-lutite facies associations of Castro Urdiales are correlated with the early Aptian volcanic episode of Gutiolo (Bilbao area). This submarine volcanic activity was associated with hydrothermal venting and nutrient flux to surface waters that gave rise to widespread glauconite formation (due to iron enrichment) and provided optimal conditions for development of oyster mass occurrences. These oxic phases were followed by disoxic/anoxic periods of calmer sea bottom conditions. The magmatic episode of Gutiolo is time equivalent to the mid-Cretaceous superplume event, responsible for the emplacement of the Ontong-Java and Manihiki Plateaus, as well as the opening of the North Atlantic through acceleration of oceanfloor spreading rates.

A new $\delta^{13}C$ curve for the Sagrado Corazón – Castro Urdiales School section has been achieved, which shows straight correlation with coeval sections of the BCB. Correlation of the $\delta^{13}C$ curve of Castro Urdiales with Aralar, Bilbao and SE France highlight the interregional extent of the OAE 1a and Aparein black-shale episodes, and could serve as a guide for future attempts to recognise similar facies/events worldwide. The marker interval at the positive CIE ($\delta^{13}C$ isotope excursion) of the late early Aptian, referenced as C7 segment in sections worldwide, postdates OAE 1a and predates the Upper Furcata Negative Excursion (UFNE).

Trends documented in this study may be used to test the extent of disoxic/anoxic episodes entouring OAE 1a, and assess the role of carbonate platform development and volcanic influence on sedimentary facies distribution in the rock record.

Data availability

Data will be made available on request.

Acknowledgements

This study is a contribution to the Basque Government Research Project IT-930-16 and the Research Group IT-1602-22 of the Basque University System. This investigation has also been supported by the University of the Basque Country (UPV/EHU) under grant number PIF18/105. The authors are grateful to J.A. Moreno-Bedmar, J.L. Latil, three anonymous reviewers and the editor of Cretaceous Research for their constructive comments and suggestions.

In memoriam – After completion of this article our dear colleague H. G. Owen passed away in March 2022. He will be greatly missed as he pioneered the identification of a vast collection of Aptian and Albian ammonites of the BCB, helping to better constrain its biostratigraphic framework. Our profound gratitude for his kindness, generosity, sharp-eye and expertise.

References

Abu-Zied, R.H., 2008. Lithostratigraphy and biostratigraphy of some Lower Cretaceous outcrops from Northern Sinai, Egypt. Cretaceous Research 29 (4), 603–624. https://doi.org/10.1016/j.cretres.2008.02.001.

Al-Ghamdi, N., Read, F.J., 2010. Facies-based sequence stratigraphic framework of the Lower Cretaceous rudist platform. Shu'aiba Formation, Saudi Arabia. In: Van Buchem, F.S.P., Al-Husseini, M.I., Maurer, F., Droste, H.J. (Eds.), Barremian-Aptian Stratigraphy and Hydrocarbon Habitat of the Eastern Arabian Plate, GeoArabia Special Publication, vol. 4 (2), pp. 367–410.

Amorosi, A., 1995. Glaucony and sequence stratigraphy: a conceptual framework of distribution in siliciclastic sequences. Journal of Sedimentary Research 65 (4b), 419–425. https://doi.org/10.1306/D4268275-2B26-11D7-8648000102C1865D.

Arthur, M.A., Sageman, B.B., 1994. Marine black shales: depositional mechanisms and environments of ancient deposits. Annual Review of Earth and Planetary Sciences 22, 499–551. https://doi.org/10.1146/annurev.ea.22.050194.002435.

Arthur, M.A., Schlanger, S.O., 1979. Cretaceous "Oceanic Anoxic Events" as causal factors in development of reef-reservoired giant oil fields. AAPG Bulletin 63 (6), 870–885. https://doi.org/10.1306/2F91848C-16CE-11D7-8645000102C1865D.

Arthur, M.A., Schlanger, S.O., Jenkyns, H.C., 1987. The Cenomanian–Turonian Oceanic Anoxic Event, II. Palaeoceanographic controls on organic-matter production and preservation. In: Brooks, J., Fleet, A. (Eds.), Marine Petroleum Source Rocks, Geological Society of London, Special Publications, vol. 26, pp. 401–420. https://doi.org/10.1144/GSL.SP.1987.026.01.25.

Beil, S., Kuhnt, W., Holbourn, A., Scholz, F., Oxmann, J., Wallmann, K., Lorenzen, J., Aquit, M., Chellai, E.H., 2020. Cretaceous oceanic anoxic events prolonged by phosphorus cycle feedbacks. Climate of the Past 16 (2), 757–782. https://doi.org/10.5194/cp-16-757-2020.

Bottini, C., Cohen, A.S., Erba, E., Jenkyns, H.C., Coe, A.L., 2012. Osmium-isotope evidence for volcanism, weathering, and ocean mixing during the early Aptian OAE 1a. Geology 40 (7), 583–586. https://doi.org/10.1130/G33140.1.

Bottini, C., Erba, E., 2018. Mid-Cretaceous paleoenvironmental changes in the western Tethys. Climate of the Past 14 (8), 1147–1163. https://doi.org/10.5194/cp-14-1147-2018.

Bottini, C., Erba, E., Tiraboschi, D., Jenkyns, H.C., Schouten, S., Sinninghe Damsté, J.S., 2015. Climate variability and ocean fertility during the Aptian Stage. Climate of the Past 11 (3), 383–402. https://doi.org/10.5194/cp-11-383-2015.

Bralower, T.J., Sliter, W.V., Arthur, M.A., Leckie, R.M., Allard, D.J., Schlanger, S.O., 1993. Dysoxic/anoxic episodes in the Aptian–Albian (Early Cretaceous). In: Pringle, M.S., Sager, W.W., Sliter, W.V., Stein, S. (Eds.), The Mesozoic Pacific: Geology, Tectonics, and Volcanism, American Geophysical Union Monograph, vol. 77, pp. 5–37.

Bralower, T.J., Arthur, M.A., Leckie, M., Sliter, W.V., Allard, D.J., Schlanger, S.O., 1994. Timing and paleoceanography of oceanic dysoxia/anoxia in the late Barremian to early Aptian (Early Cretaceous). PALAIOS 9 (4), 335–369. https://doi.org/10.2307/35150555.

Bralower, T.J., CoBabe, E., Clement, B., Slitter, W.V., Osburn, C.L., Longoria, J., 1999. The record of global change in mid-Cretaceous (Barremian-Albian) sections from the Sierra Madre, northeastern Mexico. Journal of Foraminiferal Research 29 (4), 418–437.

Bréhéret, J.G., 1997. L'Aptien et l'Albien de la fosse Vocontienne (des bordures au bassin): évolution de la sédimentation et enseignements sur les évènements anoxiques. In: Mémoires de la Société Géologique du Nord, vol. 25, p. 164. Lille.

Brovina, E.A., 2017. Planktonic foraminiferal biostratigraphy of the upper Barremian and Aptian of Crimea. Stratigraphy and Geological Correlation 25 (5), 515–531. https://doi.org/10.1134/S086959381705001X.

Castro, J.M., de Gea, G., Quijano, M.L., Aguado, R., Froehner, S., Naafs, B.D.A., Pancost, R.D., 2019. Complex and protracted environmental and ecological perturbations during OAE 1a - evidence from an expanded pelagic section from south Spain (Western Tethys). Global and Planetary Change 183, 103030. https://doi.org/10.1016/j.gloplacha.2019.103030.

Castro, J.M., Ruiz-Ortiz, P.A., de Gea, G.A., Aguado, R., Jarvis, I., Weissert, H., Molina, J.M., Nieto, L.M., Pancost, R.D., Quijano, M.L., Reolid, M., Skelton, P.W., López-Rodríguez, C., Martínez-Rodríguez, R., 2021. High-resolution C-isotope, TOC and biostratigraphic records of OAE 1a (Aptian) from an expanded hemipelagic cored succession, western Tethys: a new stratigraphic reference for global correlation and paleoenvironmental reconstruction. Paleoceanography and Paleoclimatology 36 (3), e2020PA004004. https://doi.org/10.1029/2020PA004004.

Catuneanu, O., Galloway, W.E., Kendall, C.G.St.C., Miall, A., Posamentier, H.W., Strasser, A., Tucker, M.E., 2011. Sequence stratigraphy: methodology and nomenclature. Newsletters on Stratigraphy 44 (3), 173–245. https://doi.org/10.1127/0078-0421/2011/0011.

Chambers, L.M., Pringle, M.S., Fitton, J.G., 2004. Phreatomagmatic eruptions on the Ontong Java Plateau: an Aptian $^{40}Ar/^{39}Ar$ age for volcaniclastic rocks at ODP site 1184. In: Fitton, J.G., Mahoney, J.J., Wallace, P.J., Saunders, A.D. (Eds.), Origin and Evolution of the Ontong Java Plateau, Geological Society of London, Special Publications, vol. 229, pp. 325–331. https://doi.org/10.1144/GSL.SP.2004.229.01.18.

Christie-Blick, N., 1991. Onlap, offlap and the origin of unconformity-bounded depositional sequences. Marine Geology 97 (1–2), 35–56. https://doi.org/10.1016/0025-3227(91)90018-Y.

Christie-Blick, N., Mountain, G., Miller, K., 1990. Seismic stratigraphic record of sea-level change. In: Sea-Level Change. National Academy of Sciences studies in Geophysics. National Academy Press, Washington D.C., pp. 116–140. https://doi.org/10.17226/1345

Church, J.A., Gregory, J.M., 2001. Sea-level change. In: Steele, J.H., Thorpe, S.A., Turekian, K.K. (Eds.), Encyclopedia of Ocean Sciences. Academic Press, Elsevier, pp. 2599–2604. https://doi.org/10.1006/rwos.2001.0268.

Clari, P.A., De la Pierre, F., Martire, L., 1995. Discontinuities in carbonate successions: identification, interpretation and classification of some Italian examples. Sedimentary Geology 100 (1–4), 97–121. https://doi.org/10.1016/0037-0738(95)00113-1.

Coccioni, R., Silva, I.P., Marsili, A., Verga, D., 2007. First radiation of Cretaceous planktonic foraminifera with radially elongate chambers at Angles (Southeastern France) and biostratigraphic implications. Revue de Micropaléontologie 50 (3), 215–224. https://doi.org/10.1016/j.revmic.2007.06.005.

Cohen, K.M., Finney, S.C., Gibbard, P.L., Fan, J.-X., 2013. The ICS International Chronostratigraphic Chart. Episodes 36 (3), 199–204. https://doi.org/10.18814/epiiugs/2013/v36i3/002.

Colín-García, M., Heredia, A., Cordero, G., Camprubí, A., Negrón-Mendoza, A., Ortega-Gutiérrez, F., Beraldi, H., Ramos-Bernal, S., 2016. Hydrothermal vents and prebiotic chemistry: a review. Boletin de la Sociedad Geológica Mexicana 68 (3), 599–620. https://doi.org/10.18268/BSGM2016v68n3a13.

Corfu, F., Polteau, S., Planke, S., Faleide, J.I., Svensen, H., Zayoncheck, A., Stolbov, N., 2013. U-Pb geochronology of Cretaceous magmatism on Svalbard and Franz Josef Land, Barents Sea large igneous province. Geological Magazine 150, 1127–1135. https://doi.org/10.1017/S0016756813000162.

Dröllner, M., Barham, M., Kirkland, C.L., Ware, B., 2021. Every zircon deserves a date: selection bias in detrital geochronology. Geological Magazine 158 (6), 1135–1142. https://doi.org/10.1017/S0016756821000145.

Dummann, W., Steinig, S., Hofmann, P., Lenz, M., Kusch, S., Flöge, S., Herrle, J.O., Hallmann, C., Rethemeyer, J., Kasper, H.U., Wagner, T., 2021. Driving mechanisms of organic carbon burial in the Early Cretaceous South Atlantic Cape Basin (DSDP Site 361). Climate of the Past 17 (1), 469–490. https://doi.org/10.5194/cp-17-469-2021.

Dutour, Y., 2005. Biostratigraphie, évolution et renouvellements des ammonites de l'Aptien supérieur (Gargasien) dubassin vocontien (Sud-Est de la France). Thèse Université Claude Bernard-Lyon 1, p. 302.

Erba, E., Channell, J.E.T., Claps, M., Jones, C., Larson, R.L., Opdyke, B., Premoli Silva, I., Riva, A., Salvini, G., Torricelli, S., 1999. Integrated stratigraphy of the Cismon Apticore (southern Alps, Italy); a "reference section" for the Barremian-Aptian interval at low latitudes. Journal of Foraminiferal Research 29 (4), 371–391.

Erba, E., Duncan, R.A., Bottini, C., Tiraboschi, D., Weissert, H., Jenkyns, H.C., Malinverno, A., 2015. Environmental consequences of Ontong Java Plateau and Kerguelen Plateau volcanism. In: Neal, C.R., Sager, W.W., Sano, T., Erba, E. (Eds.), The Origin, Evolution, and Environmental Impact of Oceanic Large Igneous Provinces, Geological Society of America, Special Papers, vol. 511, pp. 271–303. https://doi.org/10.1130/2015.2511(15.

Erbacher, J., Huber, B.T., Norris, R.D., Markey, M., 2001. Intensified thermohaline stratification as a possible cause for an ocean anoxic event in the Cretaceous period. Nature 409, 325–327. https://doi.org/10.1038/35053041.

Fang, P., Luo, H., Xu, B., Huber, B.T., Zhu, Y., Mu, L., 2021. Planktic foraminifera of the upper Barremian – Aptian black shale intervals from the Chaqiela section (Gamba,

southern Tibet): biostratigraphic and palaeoenvironmental implications. Cretaceous Research 127, 104934. https://doi.org/10.1016/j.cretres.2021.104934.
Fernández-Mendiola, P.A., Pérez-Malo, J., García-Mondéjar, J., 2015. Stratigraphy and facies of the Early Aptian Robayera section (Cantabria, Northern Spain). Geogaceta 58, 3–6. https://sge.usal.es/archivos/geogacetas/geo58/geo58pag3-6.pdf.
Fernández-Mendiola, P.A., Mendicoa, J., Owen, H.G., García-Mondéjar, J., 2018. The Early Aptian (Cretaceous) stratigraphy of Mount Pagasarri (N Spain): oceanic anoxic event-1a. Geological Journal 53 (5), 1802–1822. https://doi.org/10.1002/gj.3008.
Fernández-Mendiola, P.A., García-Mondéjar, J., 1989. Organización estratigráfica del Aptiense-Albiense en el sector tectosedimentario de Gorbea (Región Vasco-Cantábrica oriental). Boletín Geológico y Minero 100 (4), 116–128. https://doc.igme.es/BoletinGeoPDF/boletin%20100%20fasciculo%204.pdf.
Fernández-Mendiola, P.A., García-Mondéjar, J., Owen, H.G., 2021. Comments on "New insight on the age of the Aparein black shales in the Basque-Cantabrian Basin, northern Spain" Frau, Camille. Newsletters on Stratigraphy 54 (4), 497–499. https://doi.org/10.1127/nos/2021/0668.
Fiet, N., Quidelleur, X., Parize, O., Bulot, L.G., Gillot, P.Y., 2006. Lower Cretaceous stage durations combining radiometric data and orbital chronology: Towards a more stable relative time scale? Earth and Planetary Science Letters 246 (3–4), 407–417. https://doi.org/10.1016/j.epsl.2006.04.014.
Fluteau, F., Ramstein, G., Besse, J., Guiraud, R., Masse, J.P., 2007. The impacts of the paleogeography and sea level changes on the Mid Cretaceous climate. Palaeogeography, Palaeoclimatology, Palaeoecology 247 (3–4), 357–381. https://doi.org/10.1016/j.palaeo.2006.11.016.
Frau, C., 2021a. New insight on the age and significance of the Aparein black shales in the Basque-Cantabrian Basin, northern Spain. Newsletters on Stratigraphy 54 (1), 1–16. https://doi.org/10.1127/nos/2020/0583.
Frau, C., 2021b. New insight on the age of the Aparein black shales in the Basque-Cantabrian Basin, northern Spain –Reply to the comments made by Fernández-Mendiola et al. (2021). Newsletters on Stratigraphy 54 (4), 501–505. https://doi.org/10.1127/nos/2021/0675.
Fu, X.G., Wang, J., Wen, H.G., Wang, Z.W., Zeng, S.Q., Song, C.Y., Wang, D., Y, Nie, Y., 2020. Carbon-isotope record and paleoceanographic changes prior to the OAE 1a in the Eastern Tethys: implication for the accumulation of organic-rich sediments. Marine and Petroleum Geology 113, 104049. https://doi.org/10.1016/j.marpetgeo.2019.104049.
Ganino, C., Arndt, N.T., 2009. Climate changes caused by degassing of sediments during the emplacement of large igneous provinces. Geology 37 (4), 323–326. https://doi.org/10.1130/G25325A.1.
García-Garmilla, F., 1987. Las formaciones terrígenas del "Wealdense" y del Aptiense inferior en los anticlinorios de Bilbao y Ventoso (Vizcaya, Cantabria): estratigrafía y sedimentación. Unpublished Ph.D. thesis, Universidad del País Vasco, p. 340.
García-Mondéjar, J., 1982. El Aptiense-Albiense y Cretácico Superior de la Cuenca Vasco-Cantábrica. El Cretácico de España. Universidad Complutense de Madrid, Madrid, pp. 63–160.
García-Mondéjar, J., 1990. The Aptian–Albian carbonate episode of the Basque–Cantabrian basin (northern Spain): general characteristics, controls and evolution. In: Tucker, M.E., Wilson, J.L., Crevello, P.D., Sarg, J.F., Read, J.F. (Eds.), Carbonate Platforms: Facies, Sequences and Evolution: International Association of Sedimentologists, Special Publication, vol. 9, pp. 257–290.
García-Mondéjar, J., Fernández-Mendiola, P.A., 1993. Sequence stratigraphy and systems tracts of a mixed carbonate and siliciclastic platform-basin setting: the Albian of Lunada and Soba, northern Spain. AAPG Bulletin 77 (2), 245–275.
García-Mondéjar, J., Fernández-Mendiola, P.A., Agirrezabala, L.M., Aranburu, A., López-Horgue, M.A., Iriarte, E., Martínez-Rituerto, S., 2004. El Aptiense-Albiense de la Cuenca Vasco-Cantábrica. In: Vera, J.A. (Ed.), Geología de España. Sociedad Geológica de España – Instituto Geológico y Minero de España, Madrid, pp. 291–296.
García-Mondéjar, J., Owen, H.G., Raisossadat, N., Millán, M.I., Fernández-Mendiola, P.A., 2009. The Early Aptian of Aralar (northern Spain): stratigraphy, sedimentology, ammonite biozonation, and OAE1. Cretaceous Research 30 (2), 434–464. https://doi.org/10.1016/j.cretres.2008.08.006.
García-Mondéjar, J., Owen, H.G., Fernández-Mendiola, P.A., 2015a. Early Aptian sedimentary record and OAE1a in Cuchía (northern Spain): new data on facies and ammonite dating. Neues Jahrbuch für Geologie und Paläontologie - Abhandlungen 276, 1–26. https://doi.org/10.1127/njgpa/2015/046.
García-Mondéjar, J., Fernández-Mendiola, P.A., Owen, H.G., 2015b. The OAE1a in Cuchía (Early Aptian, Spain): C and O geochemistry and global correlation. Acta Geologica Polonica 65 (4), 525–543. https://doi.org/10.1515/agp-2015-0023.
García-Mondéjar, J., Carracedo-Sánchez, M., Owen, H.G., Fernández-Mendiola, P.A., 2019. The Early Aptian volcanic episode of Gutiolo (N Spain): expression of the Bilbao Rift Fault Zone. Geological Journal 54 (6), 3509–3526. https://doi.org/10.1002/gj.3342.
Garfunkel, Z., Katz, A., 1967. New magmatic features in Makhtesh Ramon, Southern Israel. Geological Magazine 104 (6), 608–629. https://doi.org/10.1017/S0016756800050275.
Giorgioni, M., Keller, C.E., Weissert, H., Hochuli, P.A., Bernasconi, S.M., 2015. Black shales – from coolhouse to greenhouse (early Aptian). Cretaceous Research 56, 716–731. https://doi.org/10.1016/j.cretres.2014.12.003.
Giraud, F., Pittet, B., Grosheny, D., Baudin, F., Lecuyer, C., Sakamoto, T., 2018. The palaeoceanographic crisis of the Early Aptian (OAE 1a) in the Vocontian Basin (SE France). Palaeogeography, Palaeoclimatology, Palaeoecology 511, 483–505. https://doi.org/10.1016/j.palaeo.2018.09.014.
Gold, D.P., 2021. Sea-level change in geological time. In: Alderton, D., Elias, S.A. (Eds.), Encyclopedia of Geology, second ed. Academic Press, United Kingdom, pp. 412–434. https://doi.org/10.1016/B978-0-12-409548-9.11899-8.
González-Vega, A., Fraile-Nuez, E., Santana-Casiano, J.M., González-Dávila, M., Escánez-Pérez, J., Gómez-Ballesteros, M., Tello, O., Arrieta, J.M., 2020. Significant release of dissolved inorganic nutrients from the shallow submarine volcano Tagoro (Canary Islands) based on seven-year monitoring. Frontiers in Marine Science 6, 829. https://doi.org/10.3389/fmars.2019.00829.
Gradstein, F.M., Ogg, J.G., Smith, A.G., 2004. A Geologic Time Scale 2004. Cambridge University Press, Cambridge, United Kingdom, p. 589. https://doi.org/10.1017/CBO9780511536045.
Gradstein, F.M., Agterberg, F.P., Ogg, J.G., Hardenbol, J., van Veen, P., Thierry, J., Huang, Z., 1994. A Mesozoic time scale. Journal of Geophysical Research 99 (B12), 24051–24074. https://doi.org/10.1029/94JB01889.
Gradstein, F.M., Ogg, J.G., Schmitz, M.D., Ogg, G.M., 2012. The Geologic Time Scale 2012. Elsevier, p. 1144. https://doi.org/10.1016/C2011-1-08249-8.
Gröcke, D.R., Hesselbo, S.P., Jenkyns, H.C., 1999. Carbon-isotope composition of Lower Cretaceous fossil wood: ocean-atmosphere chemistry and relation to sea-level change. Geology 27 (2), 155–158. https://doi.org/10.1130/0091-7613(1999)0273C0155:CICOLC3E2.3.CO;2.
Haq, B.U., Hardenbol, J., Vail, P.R., 1987. Chronology of fluctuating sea levels since the Triassic. Science 235 (4793), 1156–1167. https://doi.org/10.1126/science.235.4793.1156.
Hay, W.W., 2017. Toward understanding Cretaceous climate—An updated review. Science China Earth Sciences 60, 5–19. https://doi.org/10.1007/s11430-016-0095-9.
Herrle, J.O., Kößler, P., Friedrich, O., Erlenkeuser, H., Hemleben, C., 2004. High-resolution carbon isotope records of the Aptian to Lower Albian from SE France and the Mazagan Plateau (DSDP Site 545): a stratigraphic tool for paleoceanographic and paleobiologic reconstruction. Earth and Planetary Science Letters 218 (1–2), 149–161. https://doi.org/10.1016/S0012-821X(03)00646-0.
Herrle, J.O., Kößler, P., Bollmann, J., 2010. Palaeoceanographic differences of early Late Aptian black shale events in the Vocontian Basin (SE France). Palaeogeography, Palaeoclimatology, Palaeoecology 297 (2), 367–376. https://doi.org/10.1016/j.palaeo.2010.08.015.
Hillgärtner, H., 1998. Discontinuity surfaces on a shallow-marine carbonate platform (Berriasian, Valanginian, France and Switzerland). Journal of Sedimentary Research 68 (6), 1093–1108. https://doi.org/10.2110/jsr.68.1093.
Hu, X.M., Zhao, K.D., Yilmaz, I.O., Li, Y.L.X., 2012. Stratigraphic transition and palaeoenvironmental changes from the Aptian oceanic anoxic event 1a (OAE 1a) to the oceanic red bed 1 (ORB1) in the Yenicesihlar section, Central Turkey. Cretaceous Research 38, 40–51. https://doi.org/10.1016/j.cretres.2012.01.007.
Huang, C., Hinnov, L., Fischer, A.G., Grippo, A., Herbert, T., 2010. Astronomical tuning of the Aptian stage from Italian reference sections. Geology 38, 899–902. https://doi.org/10.1130/G31177.1.
Hueter, A., Huck, S., Bodin, S., Heimhofer, U., Weyer, S., Jochum, K.P., Immenhauser, A., 2019. Central Tethyan platform-top hypoxia during Oceanic Anoxic Event 1a. Climate of the Past 15 (4), 1327–1344. https://doi.org/10.5194/cp-15-1327-2019.
Hughes, G.W., 2000. Bioecostratigraphy of the Shu'aiba Formation, Shaybah field, Saudi Arabia. GeoArabia 5 (4), 545–578. https://doi.org/10.2113/geoarabia0504545.
Ibañez-Mejia, M., Pullen, A., Pepper, M., Urbani, F., Ghoshal, G., Ibañez-Mejia, J.C., 2018. Use and abuse of detrital zircon U-Pb geochronology — A case from the Río Orinoco delta, eastern Venezuela. Geology 46 (11), 1019–1022. https://doi.org/10.1130/G45596.1.
Itamar, A., Steinitz, G., 1988. Potassium-argon ages of polymetallic mineralization in the Gavnunim Valley, Makhtesh Ramon, Israel. Israel Journal of Earth Sciences 37 (2–3), 83–89.
Jenkyns, H.C., 2010. Geochemistry of oceanic anoxic events. Geochemistry, Geophysics, Geosystems 11 (3), Q03004. https://doi.org/10.1029/2009GC002788.
Jenkyns, H.C., 2018. Transient cooling episodes during Cretaceous oceanic anoxic events with special reference to OAE1a (early Aptian). Philosophical Transactions of the Royal Society A 376, 20170063. https://doi.org/10.1098/rsta.2017.0073.
Kendall, C.G.S.C., Schlager, W., 1981. Carbonates and relative changes in sea level. Marine Geology 44 (1–2), 181–212. https://doi.org/10.1016/0025-3227(81)90118-3.
Kuhnt, W., Holbourn, A., Moullade, M., 2011. Transient global cooling at the onset of early Aptian oceanic anoxic event (OAE) 1a. Geology 39 (4), 323–326. https://doi.org/10.1130/G31554.1.
Kuroda, J., Tanimizu, M., Hori, R.S., Suzuki, K., Ogawa, N.O., Tejada, M.L.G., Coffin, M.F., Coccioni, R., Erba, E., Ohkouchi, N., 2011. Lead isotopic record of Barremian–Aptian marine sediments: implications for large igneous provinces and the Aptian climatic crisis. Earth and Planetary Science Letters 307 (1–2), 126–134. https://doi.org/10.1016/j.epsl.2011.04.021.
Lang, B., Hebeda, E.H., Priem, H.N.A., 1988. K-Ar and Rb/Sr ages of Early Cretaceous magmatic rocks from Makhtesh Ramon, southern Israel. Israel Journal of Earth Sciences 37 (2–3), 65–72.
Lang, B., Steinitz, G., 1994. New $^{40}Ar/^{39}Ar$ dating of Early Cretaceous intrusive magmatics in Makhtesh Ramon. Geological Survey of Israel Current Research 9, 37–40.

Larson, R.L., Erba, E., 1999. Onset of the mid-Cretaceous greenhouse in the Barremian-Aptian: igneous events and the biological, sedimentary, and geochemical responses. Paleoceanography 14, 663–678. https://doi.org/10.1029/1999PA900040.

Le Pichon, X., Sibuet, J.C., 1971. Western extension of boundary between European and Iberian plates during the Pyrenean orogeny. Earth and Planetary Science Letters 12 (1), 83–88. https://doi.org/10.1016/0012-821X(71)90058-6.

Lehmann, J., Friedrich, O., von Bargen, D., Hemker, T., 2012. Early Aptian bay deposits at the southern margin of the Lower Saxony Basin: Integrated stratigraphy, palaeoenvironment and OAE 1a. Acta Geologica Polonica 62 (1), 35–62. https://doi.org/10.2478/v10263-012-0002-2.

Li, Y.-X., Bralower, T.J., Montañez, I.P., Osleger, D.A., Arthur, M.A., Bice, D.M., Herbert, T.D., Erba, E., Premoli Silva, I., 2008. Toward an orbital chronology for the early Aptian Oceanic Anoxic Event (OAE1a, ~ 120 Ma). Earth and Planetary Science Letters 271 (1–4), 88–100. https://doi.org/10.1016/j.epsl.2008.03.055.

Malod, J.A., Mauffret, A., 1990. Iberian plate motions during the Mesozoic. Tectonophysics 184 (3–4), 261–278. https://doi.org/10.1016/0040-1951(90)90443-C.

Marsaglia, K.M., 2005. Sedimentology, petrology, and volcanology of the lower Aptian Oceanic Anoxic Event (OAE1a), Shatsky Rise, north-central Pacific Ocean. In: Bralower, T.J., Premoli Silva, I., Malone, M.J. (Eds.), Proceedings of the Ocean Drilling Program – Scientific Results 198 [Online]. https://doi.org/10.2973/odp.proc.sr.198.109.2005.

Matsumoto, H., Coccioni, R., Frontalini, F., Shirai, K., Jovane, L., Trindade, R., Savian, J.F., Tejada, M.L., Gardin, S., Kuroda, J., 2021. Long-term Aptian marine osmium isotopic record of Ontong Java Nui activity. Geology 49 (9), 1148–1152. https://doi.org/10.1130/G48863.1.

Méhay, S., Keller, C.E., Bermasconi, S.M., Weissert, H., Erba, E., Bottini, C., Hochuli, P.A., 2009. A volcanic CO2 pulse triggered the Cretaceous oceanic anoxic event 1a and a biocalcification crisis. Geology 37 (9), 819–822. https://doi.org/10.1130/G30100A.1.

Menegatti, A.P., Weissert, H.J., Brown, R.S., Tyson, R.V., Farrimond, P., Strasser, A., Caron, M., 1998. High-resolution $\delta^{13}C$ stratigraphy through the Early Aptian "Livello Selli" of the Alpine Tethys. Paleoceanography and Paleoclimatology 13 (5), 530–545. https://doi-org.ehu.idm.oclc.org/10.1029/98PA01793.

Midtkandal, I., Svensen, H.H., Planke, S., Corfu, F., Polteau, S., Torsvik, T.H., Grundväg, S.A., Selnes, H., Kürschner, W., Olaussen, S., 2016. The Aptian (Early Cretaceous) oceanic anoxic event (OAE1a) in Svalbard, Barents Sea, and the absolute age of the Barremian-Aptian boundary. Palaeogeography, Palaeoclimatology, Palaeoecology 463, 126–135. https://doi.org/10.1016/j.palaeo.2016.09.023.

Millán, M.I., Weissert, H.J., Fernández-Mendiola, P.A., García-Mondéjar, J., 2009. Impact of Early Aptian carbon cycle perturbations on evolution of a marine shelf system in the Basque-Cantabrian Basin (Aralar, N Spain). Earth and Planetary Science Letters 287 (3–4), 392–401. https://doi.org/10.1016/j.epsl.2009.08.023.

Millán, M.I., Weissert, H.J., López-Horgue, M.A., 2014. Expression of the late Aptian cold snaps and the OAE1b in a highly subsiding carbonate platform (Aralar, northern Spain). Palaeogeography, Palaeoclimatology, Palaeoecology 411, 167–179. https://doi.org/10.1016/j.palaeo.2014.06.024.

Miller, K.G., Kominz, M.A., Browning, J.V., Wright, J.D., Mountain, G.S., Katz, M.E., Sugarman, P.J., Cramer, B.S., Christie-Blick, N., Pekar, S.F., 2005. The Phanerozoic Record of Global Sea-Level Change. Science 310 (5752), 1293–1298. https://doi.org/10.1126/science.1116412.

Montadert, L., Roberts, D.G., De Charpal, O., Guennoc, P., 1979. Rifting and subsidence of the northern continental margin of the Bay of Biscay. Initial Reports of the Deep Sea Drilling Project 48, 1025–1059.

Moreno-Bedmar, J.A., Company, M., Bover-Arnal, T., Salas, R., Delanoy, G., Martínez, R., Grauges, A., 2009. Biostratigraphic characterization by means of ammonoids of the lower Aptian Oceanic Anoxic Event (OAE 1a) in the eastern Iberian Chain (Maestrat Basin, eastern Spain). Cretaceous Research 30 (4), 864–872. https://doi.org/10.1016/j.cretres.2009.02.004.

Moreno-Bedmar, J.A., Company, M., Sandoval, J., Tavera, J.M., Bover-Arnal, T., Salas, R., Delanoy, G., Maurrasse, F.J.-M.R., Martínez, R., 2012. Lower Aptian ammonite and carbon isotope stratigraphy in the eastern Prebetic Domain (Betic Cordillera, southeastern Spain). Geológica Acta 10 (4), 333–350. https://doi.org/10.1344/105.000001752.

Moullade, M., Kuhnt, W., Bergen, J.A., Masse, J.P., Tronchetti, G., 1998. Correlation of biostratigraphic and stable isotope events in the Aptian historical stratotype of La Bédoule (SE France). Comptes Rendus de l'Academie des Sciences - Series IIA: Earth and Planetary Science 327 (10), 693–698. https://doi.org/10.1016/S1251-8050(99)80027-5.

Moullade, M., Tronchetti, G., Bellier, J.P., 2008. Associations et biostratigraphie des Foraminifères benthiques et planctoniques du Bédoulien sommital et du Gargasien inférieur de La Tuilière - St-Saturnin-lès-Apt (aire stratotypique de l'Aptien, Vaucluse, SE France). Carnets de Géologie [Notebooks on Geology], Brest. Article 2008/01 (CG2008-A01).

Moullade, M., Tronchetti, G., 2010. A preliminary quantitative study of Foraminifera within the paleoenvironmental record of the Aptian stratotypes. Revue de Micropaléontologie 53 (3), 193–208. https://doi.org/10.1016/j.revmic.2010.01.001.

Naafs, B.D.A., Pancost, R.D., 2016. Sea-surface temperature evolution across Aptian Oceanic Anoxic Event 1a. Geology 44 (11), 959–962. https://doi.org/10.1130/G38575.1.

Naafs, B.D.A., Castro, J.M., De Gea, G.A., Quijano, M.L., Schmidt, D.N., Pancost, R.D., 2016. Gradual and sustained carbon dioxide release during Aptian oceanic anoxic event 1a. Nature Geoscience 1–5. https://doi.org/10.1038/ngeo2627.

Najarro, M., Rosales, I., Moreno-Bedmar, J.A., de Gea, G.A., Barrón, E., Company, M., Delanoy, G., 2011. High-resolution chemo- and biostratigraphic records of the Early Aptian oceanic anoxic event in Cantabria (N Spain): palaeoceanographic and palaeoclimatic implications. Palaeogeography, Palaeoclimatology, Palaeoecology 299, 137–158. https://doi.org/10.1016/j.palaeo.2010.10.042.

Nelson, A.R., 2013. Sea-levels, Late Quaternary: Tectonics and Relative Sea-Level Change. In: Elias, S.A., Mock, C.J. (Eds.), Encyclopedia of Quaternary Science, second ed., pp. 503–519. https://doi.org/10.1016/B978-0-444-53643-3.00141-2.

Núñez-Useche, F., Moreno-Bedmar, J.A., Company, M., Barragán, R., 2014. A negative carbon isotope excursion within the *Dufrenoyia furcata* Zone: proposal for a new episode for chemostratigraphic correlation in the Aptian. Carnets de Géologie [Notebooks on Geology] 14, 129–137. https://doi.org/10.4267/2042/53734.

Odin, G.S., Matter, A., 1981. De glauconiarum origine. Sedimentology 28 (5), 611–641. https://doi.org/10.1111/j.1365-3091.1981.tb01925.x.

Odin, G.S., Fullagar, P.D., 1988. Geological significance of the glaucony facies. In: Odin, G.S. (Ed.), Green Marine Clays Oolitic Ironstone Facies, Verdine Facies, Glaucony Facies and Celadonite-Bearing Facies — A Comparative Study. Elsevier, Amsterdam, pp. 295–332. https://doi.org/10.1016/S0070-4571(08)70069-4.

Ogg, J.G., Ogg, G.M., Gradstein, F.M., 2016. A Concise Geologic Time Scale: 2016. Elsevier, Amsterdam, p. 234.

Ohkouchi, N., Kuroda, J., Taira, A., 2015. The origin of Cretaceous black shales: a change in the surface ocean ecosystem and its triggers. Proceedings of the Japan Academy, Series B 91 (7), 273–291. https://doi.org/10.2183/pjab.91.273.

Olierook, H.K.H., Jourdan, F., Merle, R.E., 2019. Age of the Barremian–Aptian boundary and onset of the Cretaceous Normal Superchron. Earth-Science Reviews 197, 102906. https://doi.org/10.1016/j.earscirev.2019.102906.

Pancost, R.D., Crawford, N., Magness, S., Turner, A.D., Jenkyns, H.G., Maxwell, J.R., 2004. Further evidence for the development of photic-zone euxinic conditions during Mesozoic Oceanic Anoxic Events. Journal of the Geological Society 161 (3), 353–364. https://doi.org/10.1144/0016764903-059.

Pascal, A., 1985. Les systèmes biosédimentaires urgoniens (Aptien-Albien) sur la marge Nord Ibérique. In: Mémoires géologiques de l'Université de Dijon, vol. 10, p. 561.

Pedersen, T.F., Calvert, S.E., 1990. Anoxia vs. productivity: what controls the formation of organic-carbon-rich sediments and sedimentary rocks? AAPG Bulletin 74 (4), 454–466. https://doi.org/10.1306/0C9B232B-1710-11D7-8645000102C1865D.

Pérez-Malo, J., Fernández-Mendiola, P.A., García-Mondéjar, J., 2017. Facies analysis and stratigraphy of the Suances Upper Albian carbonate platform (Northern Spain). Geogaceta 61, 147–150. https://sge.usal.es/archivos/geogacetas/geo61/geo61_37p147_150.pdf.

Polteau, S., Hendriks, B.W.H., Planke, S., Ganerød, M., Corfu, F., Faleide, J.I., Midtkandal, I., Svensen, H.S., Myklebust, R., 2016. The Early Cretaceous Barents Sea sill complex: distribution, $^{40}Ar/^{39}Ar$ geochronology, and implications for carbon gas formation. Palaeogeography, Palaeoclimatology, Palaeoecology 441 (1), 83–95. https://doi.org/10.1016/j.palaeo.2015.07.007.

Quijano, M.L., Castro, J.M., Pancost, R.D., De Gea, G.A., Najarro, M., Aguado, R., Rosales, I., Chivelet, J.M., 2012. Organic geochemistry, stable isotopes, and facies analysis of the Early Aptian OAE — New records from Spain (Western Tethys). Palaeogeography, Palaeoclimatology, Palaeoecology 365–366, 276–293. https://doi.org/10.1016/j.palaeo.2012.09.033.

Rat, P., 1988. The Basque–Cantabrian Basin between the Iberian and European plates: some facts but still many problems. Revista Sociedad Geológica de España 1 (3–4), 327–348.

Reboulet, S., Szives, O., Aguirre-Urreta, B., Barragán, R., Company, M., Idakieva, V., Ivanov, M., Kakabadze, M.V., Moreno-Bedmar, J.A., Sandoval, J., Baraboshkin, E.J., Caglar, M.K., Fozy, I., Gonzalez-Arreola, C., Kenjo, S., Lukeneder, A., Raisossadat, S.N., Rawson, P.F., Tavera, J.M., 2014. Report on the 5th International Meeting of the IUGS Lower Cretaceous Ammonite Working Group, the Kilian Group (Ankara, Turkey, 31st August 2013). Cretaceous Research 50, 126–137. https://doi.org/10.1016/j.cretres.2014.04.001.

Reolid, M., Abad Martínez, I., 2014. Glauconitic laminated crusts from hydrothermal alteration of Jurassic pillow-lavas (Betic Cordillera, S Spain): a microbial influence case. Journal of Iberian Geology 40 (3), 389–408. https://doi.org/10.5209/rev_JIGE.2014.v40.n3.43080.

Rosales, I., Fernández-Mendiola, P.A., García-Mondéjar, J., 1994. Carbonate depositional sequence development on active fault blocks: the Albian in the Castro Urdiales area, northern Spain. Sedimentology 41 (5), 861–882. https://doi.org/10.1111/j.1365-3091.1994.tb01429.x.

Rosales, I., 1995. La plataforma carbonatada de Castro Urdiales (Aptiense-Albiense, Cantabria). Unpublished Ph.D. thesis, Universidad del País Vasco, p. 496.

Rosales, I., 1999. Controls on carbonate-platform evolution on active fault blocks; the Lower Cretaceous Castro Urdiales Platform (Aptian-Albian, northern Spain). Journal of Sedimentary Research 69 (2), 447–465. https://doi.org/10.2110/jsr.69.447.

Ryan, W.B.F., Cita, M.B., 1977. Ignorance concerning episodes of ocean-wide stagnation. Developments in Sedimentology 23, 197–215. https://doi.org/10.1016/S0070-4571(08)70558-2.

Santana-Casiano, J.M., González-Dávila, M., Fraile-Nuñez, E., 2017. The emissions of the Tagoro submarine volcano (Canary Islands, Atlantic Ocean): effects on the physical and chemical properties of the seawater. In: Aiello, G. (Ed.), Volcanoes: Geological and Geophysical Setting, Theoretical Aspects and Numerical Modeling, Applications to Industry and Their Impact on the Human Health. IntechOpen, pp. 53–72. https://doi.org/10.5772/intechopen.70422.

Sarg, J.F., 1988. Carbonate sequence stratigraphy. In: Wilgus, C.K., Hastings, B.S., Posamentier, H., Van Wagoner, J., Ross, C.A., Kendall, C.G.St.C. (Eds.), Sea-level Changes: an Integrated Approach, SEPM Society for Sedimentary Geology, Special Publication, vol. 42, pp. 155–181. https://doi.org/10.2110/pec.88.01.0155.

Sattler, U., Immenhauser, A., Hillgärtner, H., Esteban, M., 2005. Characterization, lateral variability and lateral extent of discontinuity surfaces on a Carbonate Platform (Barremian to Lower Aptian, Oman). Sedimentology 52 (2), 339–361. https://doi.org/10.1111/j.1365-3091.2005.00701.x.

Schlager, W., Reijmer, J.J.G., Droxler, A., 1994. Highstand shedding of carbonate platforms. Journal of Sedimentary Research 64 (3b), 270–281. https://doi.org/10.1306/D4267FAA-2B26-11D7-8648000102C1865D.

Schlanger, S.O., Jenkyns, H.C., 1976. Cretaceous oceanic anoxic events: causes and consequences. Geologie en Mijnbouw 55 (3–4), 179–184.

Scholle, P.A., Arthur, M.A., 1980. Carbon isotope fluctuations in Cretaceous pelagic limestones: potential stratigraphic and petroleum exploration tool. AAPG Bulletin 64 (1), 67–87. https://doi.org/10.1306/2F91892D-16CE-11D7-8645000102C1865D.

Sotomayor-García, A., Rueda, J.L., Sánchez-Guillamón, O., Urra, J., Vázquez, J.T., Fernández-Salas, L.M., López-González, N., González-Porto, M., Santana-Casiano, J.M., González-Dávila, M., Presas-Navarro, C., Fraile-Nuez, E., 2019. First macro-colonizers and survivors around Tagoro submarine volcano, Canary Islands, Spain. Geosciences 9 (1), 52. https://doi.org/10.3390/geosciences9010052.

Svensen, H., Fristad, K.E., Polozov, A.G., Planke, S., 2015. Volatile generation and release from continental large igneous provinces. In: Schmidt, A., Fristad, K.E., Elkins-Tanton, L. (Eds.), Volcanism and Global Environmental Change. Cambridge University Press, Cambridge, pp. 177–192.

Tarduno, J.a., Sliter, W.V., Kroenke, L., Leckie, M., Mayer, H., Mahoney, J.J., Musgrave, R., Storey, M., Winterer, E.L., 1991. Rapid formation of Ontong java plateau by Aptian mantle plume volcanism. Science 80 (254), 399–403. https://doi.org/10.1126/science.254.5030.399.

Tendil, A.J.B., Frau, C., Léonide, P., Fournier, F., Borgomano, J.R., Lanteaume, C., Masse, J.P., Rolando, J.P., 2019. Stable-isotope chemostratigraphy of Urgonian-type platform carbonates: time to be cautious? Stratigraphy & Timescales 4, 165–216. https://doi.org/10.1016/bs.sats.2019.08.001.

Tejada, M.L.G., Suzuki, K., Kuroda, J., Coccioni, R., Mahoney, J.J., Ohkouchi, N., Sakamoto, T., Tatsumi, Y., 2009. Ontong Java Plateau eruption as a trigger for the early Aptian oceanic anoxic event. Geology 37 (9), 855–858. https://doi.org/10.1130/G25763A.1.

Timm, C., Hoernle, K., Werner, R., Hauff, F., van den Bogaard, P., Michael, P., Coffin, M.F., Koppers, A., 2011. Age and geochemistry of the oceanic Manihiki Plateau, SW Pacific: new evidence for a plume origin. Earth and Planetary Science Letters 304 (1–2), 135–146. https://doi.org/10.1016/j.epsl.2011.01.025.

Toscano, A.G., Lazo, D.G., Luci, L., 2018. Taphonomy and paleoecology of Lower Cretaceous oyster mass occurrences from west-central Argentina and evolutionary paleoecology of gregariousness in oysters. PALAIOS 33 (6), 237–255. https://doi.org/10.2110/palo.2017.096.

Vail, P.R., Mitchum Jr., R.M., Thompson III, S., 1977. Seismic stratigraphy and global changes of sea level: Part 4. Global cycles of relative changes of sea level: Section 2. Application of seismic reflection configuration to stratigraphic interpretation. In: Payton, C.E. (Ed.), Seismic Stratigraphy – Applications to Hydrocarbon Exploration, AAPG Memoir, vol. 26, pp. 83–97. https://doi.org/10.1306/M26490C6.

Vogt, P.R., 1989. Volcanogenic upwelling of anoxic, nutrient-rich water: a possible factor in carbonate-bank/reef demise and benthic faunal extinctions? Geological Society of America Bulletin 101 (1), 1225–1245. https://doi.org/10.1130/0016-7606(1989)1013C1225:VUOANR3E2.3.CO;2.

Wang, P.J., Chen, C.Y., Liu, H.B., 2016. Aptian giant explosive volcanic eruptions in the Songliao Basin and Northeast Asia: a possible cause for global climate change and OAE-1a. Cretaceous Research 62, 98–108. https://doi.org/10.1016/j.cretres.2015.09.021.

Weissert, H., Erba, E., 2004. Volcanism, CO2 and palaeoclimate: a Late Jurassic – Early Cretaceous carbon and oxygen isotope record. Journal of the Geological Society 161 (4), 695–702. https://doi.org/10.1144/0016-764903-087.

Weissert, H.J., Lini, A., 1991. Ice age interludes during the time of Cretaceous Greenhouse climate? In: Mueller, D.W., McKenzie, J.A., Weisser, H. (Eds.), Controversies in Modern Geology: Evolution of Geological Theories in Sedimentology, Earth History and Tectonics. Academic Press, London, pp. 173–191.

Weissert, H., Lini, A., Föllmi, K.B., Kuhn, O., 1998. Correlation of Early Cretaceous carbon isotope stratigraphy and platform drowning events: a possible link? Palaeogeography, Palaeoclimatology, Palaeoecology 137 (3–4), 189–203. https://doi.org/10.1016/S0031-0182(97)00109-0.

Westermann, S., Stein, M., Matera, V., Fiet, N., Fleitmann, D., Adatte, T., Föllmi, K.B., 2013. Rapid changes in the redox conditions of the western Tethys Ocean during the early Aptian oceanic anoxic event. Geochimica et Cosmochimica Acta 121, 467–486. https://doi.org/10.1016/j.gca.2013.07.023.

Wilson, J.L., 1967. Cyclic and reciprocal sedimentation in Virgilian strata of southern New Mexico. Geological Society of America Bulletin 78 (7), 805–818. https://doi.org/10.1130/0016-7606(1967)78[805:CARSIV]2.0.CO;2.

Zhang, Y., Ogg, J.G., Minguez, D., Hounslow, M.W., Olaussen, S., Gradstein, F.M., Esmeray-Senlet, S., 2021. Magnetostratigraphy of U-Pb–dated boreholes in Svalbard, Norway, implies that magnetochron M0r (a proposed Barremian-Aptian boundary marker) begins at 121.2 ± 0.4 Ma. Geology 49 (6), 733–737. https://doi.org/10.1130/G48591.1.

Appendix A. Supplementary data

Supplementary data to this article can be found online at https://doi.org/10.1016/j.cretres.2022.105430.